

國立交通大學
電機與控制工程學系
博士論文

發展以小波為基礎的禪定腦電波詮釋方法

Wavelet-Based Methods Developed for Interpreting
The Zen Meditation EEG



研究生：張剛鳴

指導教授：羅佩禎

中華民國九十五年一月

發展以小波為基礎的禪定腦電波詮釋方法

中文摘要

禪定學 (Meditation) 是目前新興的另類輔助醫學 (CAM) 研究中非常重要且熱門的研究領域。禪定對於身心健康有很大幫助，尤其是關於壓力調適、血壓控制、情緒管理、防止老化、增強免疫力等許多導致慢性疾病的因素有改善，而這些均深深影響現代人健康，尤其影響政府的健康保險費用支出。另一方面禪定是一種非侵入式的活動，練習者只需要依照正確的指導，循序漸進的學習，就會有身心的改善。尤其本文以禪宗印心佛法修練者為受測對象，因為在此團體中，有許多人確實透過禪修而獲致多方面益處，諸如舒解壓力、身心健康、人格穩定、潛能開發、提昇學習與工作績效…等；對於目前台灣沉重的健保負擔及國人身心健康品質，相信得以提供一個很好的解決之道。

本論文主要貢獻在於 (第一篇論文) 以通訊與系統理論來了解並詮釋禪修對於身心狀況與生命特質的改變機制，並以共振理論來解說加持能量對腦電波的影響。所發表之論文中，有報告統計調查結果 (第二篇論文)，並且針對禪坐時的腦電波變化，發展出以小波為基礎，結合模糊分群法的 DSP 訊號演算詮釋法則 (第三篇論文)。演算法之於禪坐腦電波變化的量化效能也充分得到驗證，並進而應用於詮釋腦電波型態與長時間禪坐腦電波劇本。

本論文中針對人體在禪定練習過程中，另外發展以小波及赫斯特指數的演算法，以便有效鑑別腦電波的 beta 波 (第四篇論文)，而 beta 波是禪定者感受到「內在光」(inner light) 時出現的腦波。禪定者 beta 波出現比例愈高者，視覺誘發電位振幅同時有減少的趨勢(控制組則是振幅增長)，顯示禪定時視覺傳導系統不易受到外界視

覺刺激而變化(第五篇論文)。結合受測者口述統計、腦電波及視覺誘發電位的數據，可間接說明”內在光”存在的生理機制，這點與實際禪定練習者經驗及相關文獻所記載的「內在光」的各宗教共通經驗不謀而合。這項禪定時受測者大腦有光刺激反應的模型，是第一次相關研究中所提出的假說。



ABSTRACT

Meditation is an important topic on complementary and alternative medicine (CAM), the newly developed and fast growing research area. Meditation has significant improvement effects on health, especially on the subjects with pressure, hypertension, emotional control, anti-aging, immune system enhancement, that are critical factors on modern illness and government expenditure on health insurance. Meditation is also highly valued due to the non-invasive properties; practitioners can achieve physical and spiritual achievements by correct teaching and constantly practicing. Zen Meditation practitioners who are subjects of this research especially gain many profits from meditation practicing, they are good at moderate their emotions, stresses, and they have more stable personality, higher learning and working performances. Meditation is a very good solution to people's health and heavy burdens of Taiwan's health insurance budgets.

The first major contribution of this thesis is to interpret the dynamic mechanism of health and spirit under Zen meditation by communication and system theories, and explain the EEG change under blessing by circuit resonance theory. We also develop a meditation EEG interpretation principle based on wavelet features and Fuzzy C-means clustering to investigate meditation EEG types and long term meditation EEG scenarios. The entire proposed algorithm's performances are tested by simulated and real EEG signals.

We also developed a Hurst exponent based method to identify beta EEG rhythms, that is the specific EEG patterns when practitioners feeling the "inner light" during meditation.

The little variation of F-VEP amplitude during Zen meditation reflects a more stable visual perceptive system during Zen meditation that is contrary to the visual response of the control subjects under eye-closed relaxation. The subject's narration and VEP, EEG data prevail the possibility of "inner light", and "inner light" are match the practitioners' experience and many religious references. The visual response model of "inner light" is the first hypothesis proposed in the academic report.



Contents

Table Index	9
Figure Index	10
Chapter 1 INTRODUCTION	12
1.1 Introduction of Zen Meditation	12
1.2 Survey of literature on the meditation research	17
Chapter 2 METHODS	19
2.1 Introduction of Biomedical signals	19
2.1.1 Introduction of EEG	19
2.1.2 Introduction of VEP	22
2.2 Data Recording Procedures	23
2.2.1 Health survey	23
2.2.2 Blessing	24
2.2.3 Meditation EEG Scenarios	27
2.2.4 VEP	28
2.3 Signal processing algorithms	29
2.3.1 Wavelet approach	29
2.3.2 Sub-Band Power	32
2.3.3 FCM clustering	33
2.3.4 FCM-merging strategies	36



2.3.5 Hurst exponent	42
2.3.6 Alpha-suppressed EEG identification	44
2.3.7 VEP waveform feature extraction	46
Chapter 3 RESULTS	49
3.1 Health Survey	49
3.1.1 Experiences of Zen practitioners	49
3.1.2 Psychological and mental health of the experimental subjects	51
3.1.3 Physiological health conditions in the experimental group	56
3.2 EEG alpha blocking during Zen meditation	62
3.3 Blessing --significant alpha blocking during blessings	64
3.4 Meditation EEG Scenarios	68
3.4.1 FCM and Wavelet	68
3.4.2 Hurst exponent	76
3.5 Correlation between VEP and alpha-suppressed EEG	81
3.5.1 Alpha-suppressed EEG	81
3.5.2 F-VEP	84



3.5.3 Feature space of EEG and F-VEP	87
Chapter 4 DISCUSSION AND CONCLUSION	89
4.1 Effect of Zen meditation on health	90
4.2 Principle of blessings	91
4.3 Meditation EEG patterns and meditation scenarios	93
4.4 Inner-light nature of Zen meditation practice	94
REFERENCES	96
Appendix-A: original survey questionnaires (Chinese version)	111

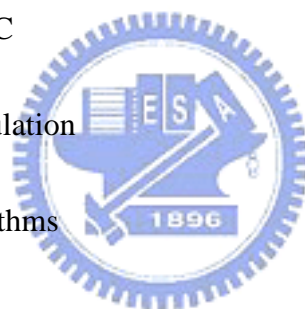


Table Index

1.1	Some examples showing meditation as an effective medical therapy	16
2.1	EEG rhythmic bands and the corresponding wavelet filter bands	32
3.1	Distribution of the meditation lengths for each meditation position	51
3.2	Results of self evaluation of the daily frame of mind	53
3.3	Statistics of HIC applications in the experimental group of 860 subjects	58
3.4	The average HIC applications of different ages and genders	59
3.5	Average number of HIC applications of the experimental subjects	61
3.6	Subband wavelet power of five prototypes in meditation EEG	73
3.7	Corresponding H, SSE, and mean amplitude of each EEG segments	79
3.8	H and SSE distribution of 200 EEG epochs	79
3.9	F-VEP peak amplitude difference with control and experimental groups.	86

Figure Index:

1	EEG electrodes displacement according to 10-20 system	21
2	Typical VEP patterns	23
3	Some important apertures (Chakras) in Zen meditation	26
4	Illustration of wavelet decomposition of an EEG segment	31
5	Block diagram of FCM-merging strategies	33
5(b)	Flowchart of cluster-merge A	37
5(c)	Flowchart of cluster-merge B	40
5(d)	Flowchart of cluster-merge C	42
6	Chart of H&SSE pairs calculation	45
7	F-VEP preprocessing algorithms	47
8	F-VEP trial stacking map	48
9	Histogram of contentment and stress moderation (weekly practicing frequencies)	54
10	Histogram of contentment and stress moderation (practicing years)	54
11	Histogram of stress moderation (weekly practicing frequencies)	55
12	Histogram of stress moderation (practicing years)	56
13	Histogram of contentment (weekly practicing frequencies)	56
14	Histogram of contentment (practicing years)	57
15	The average HIC applications of different ages and genders	58
16	Effect of weekly practicing frequency on the physiological health	62



17	Effect of practicing years on the physiological health	62
18	EEG segment of subject when perceiving the light	64
19	Three EEG segments reflecting the effect of perceiving the light	65
20	Running power-percentage analysis for the blessing EEG data	66
21	Running power-percentage analysis for the non-blessing EEG data	68
22	Distribution of subband wavelet coefficient powers (v_7 , v_6 , v_5 , and v_4)	70
23	Three-dimensional illustration of wavelet feature vector $\{v_5[\cdot], v_6[\cdot], v_7[\cdot]\}$	71
24	Five meditation-EEG patterns (from top): Δ , $\Delta+\theta$, $\theta+\underline{\alpha}$, α^+ , and Φ	72
25	Five meditation scenarios based on evolution of meditation EEG	75
26	Time-domain EEG segments of the H&SSE pairs	78
27	The Fourier spectrums of the EEG waveforms	79
28	H&SSE pairs' distribution of long-term EEG rhythms	81
29	Typical alpha-suppressed EEG segment and corresponding FFT spectrum	83
30	Illustration of sum-versus-max alpha-suppressed EEG duration	84
31	Average percentages of alpha-suppressed EEG	85
32	Average F-VEP patterns recorded during three recording sessions	86
33	Maximum alpha-suppressed EEG duration versus F-VEP N3-P2 peak amplitude differences of Session II and I	89

Chapter 1 INTRODUCTION

1.1 Introduction of Zen Meditation

As the complementary and alternative medicine (CAM) becomes more appealing to the public, researchers begin taking a more serious attitude toward this oriental approach for health maintenance and promotion [1]-[3].

According to the definition of National Center for Complementary and Alternative Medicine (NCCAM) [4], a division of the National Institutes of Health of USA, complementary and alternative medicine is a group of diverse medical and health care systems, practices, and products that are not presently considered to be part of conventional medicine. NCCAM also classified the CAM into five categories, which are (1) Alternative Medical Systems, (2) Mind-Body Interventions, (3) Biologically Based Therapies, (4) Manipulative and Body-Based Methods, and (5) Energy Therapies. This paper's focus, meditation, is belonging to the Mind-Body interventions categories. NCCAM defines Mind-Body Interventions categories as a variety of techniques designed to enhance the mind's capacity to affect bodily function and symptoms. For example: patient support groups, cognitive-behavioral therapy, meditation, prayer, mental healing, and therapies that use creative outlets such as art, music, or dance.

Due to the fact that more Zen-meditation practitioners have proved the benefit of Zen meditation to health, our research group thus attempted to explore the human life-system

model under meditation since 1998. In this research work, we mainly focus on the electrophysiological signals, including the electroencephalograph (EEG), electrocardiograph (ECG), visual evoked potential (VEP), blood pressure wave (BPW), and galvanometric skin resistance (GSR), with the reference of some CAM (complementary and alternative medicine) instruments. Although a number of Zen-meditation sects have emerged, orthodox Zen-Buddhist meditation is the only approach acceding to the essence of Buddha Shakyamuni. Zen-Buddhist practice has become not only the religion but also greatly improved physical and mental health.

Zen-Buddhism originated about 2,500 years ago. The practice was handed down by Buddha Shakyamuni to the Great Kashiya. The same path towards Buddhahood was promulgated to mainland China in 527 by the 28th patriarch Bodhidharma. Until the 33th patriarch Huei-Neng, Zen-Buddhist practice began reaching to other areas such as Japan and Taiwan. The current patriarch is Zen master Wu Jue Miao Tian, the 85th patriarch of the orthodox Zen-Buddhism Sect.

The core essence of Zen-Buddhist is practice rather than Sutra-texts studying. Through meditation, a practitioner seeks to attain the enlightened state of spiritual release from the Self [5]-[6]. In the history of orthodox Zen-Buddhism, very few disciples were able to catch its quintessence since it cannot be taught in any form of lecture. Written material and spoken words cannot pass on the true message of Zen. Although there are a few sects

derived from Zen Buddhism, they cannot be true Zen without succession to the supreme wisdom and the noumenal energy.

According to the experiences described by meditators, in the course of Zen meditation, meditators transcend the physiological (the fifth), mental (the sixth), and subconscious (the seventh) states and attain the Alaya (the eighth) conscious state [6]. Under Zen meditation they gradually release their minds from their physical and mental sensors, leave off the messages from the outside world, and keep subliminal consciousness tranquil. In addition, in meditative states, meditators find that their bodies are filled with inner energy, and they perceive an inner light [5]: the original, true self — discover and uncover the light of eternal life.



Inner energy differs from qi energy [7]-[9]. As stated by practitioners, qi energy can be ranked into 4 levels: real qi, spiritual qi, electrical qi, and light qi. Qigong practitioners mostly achieve the real-qi level, which belongs to the physical world and, accordingly, is time-varying. The highest level achieved by qigong practitioners is the spiritual qi. Even reaching this level, one still cannot prove the true self. The spiritual qi can be transformed, via orthodox Zen-Buddhist practice, into electrical qi and even light qi that is finally the light of eternal life.

Although the inner energy is an inconceivable, supernatural power, it is not merely a conceptual or hypothetical entity. The most effective way to experience the inner energy is

meditation. The procedures to practice Zen meditation include: (1) sit with legs crossed (lotus position), (2) regulate the respiration, (3) concentrate on the Chakra, and finally relieve all thoughts and mental activities. The practitioner can explore the inner energy by transcending the physiological, mental, subconscious, and Alaya conscious states. During the Zen meditation course, blessing power bestowed by the Master attaining Buddhahood will aid to the inner energy experience of the disciples. The human life system in this state may be interpreted as follows: one shuts off his physical and mental sensors, disables the message transmission from the outside world, and is finally freed from the interference of the subconscious. In the physical world, the human life system lives in the domain of physical, mental, and even subconscious activities. Nevertheless, a message originating or conveyed in this domain, to our true self, behaves like the dark cloud covering the brilliance of the sunlight. Speaking in the engineering sense, the signal is contaminated by noise.

Zen-Buddhist practitioners have discovered that the inner energy is the resource of health and bliss. According to our investigation, the practitioners through years of Zen-Buddhist practice can change the constitution of their bodies by ignition of the inner energy. A large number of practitioners are found not only to maintain better health but also to remain younger and more energetic than normal people do (Table 1.1).

In this thesis, we investigated the effects and phenomena of Zen meditation by (1) the particularly formulated questionnaire survey, and (2) analysis of biomedical signals (EEG,

Table 1.1. Some examples showing meditation as an effective medical therapy (November 2001)

Case ^a	Before	After
Y.-H. Hsueh (Mr.) 37, 6	Chronic Hepatitis B in 1994: surface fibrosis of liver, GPT ^b =205, palpitation, insomnia	Normal liver surface, GPT=21, no more palpitation and insomnia
M.-H. Lin (Mrs.) 50, 3	Rectal cancer in 1998 (no other treatment after surgery)	Healthy, no evidence of relapse
S.-C. Lo (Mr.) 32, 10	Spontaneous pneumothorax since teenager	Complete recovery
T. Yu (Mr.) 48, 8	Severe palpitation and high blood pressure (>210mmHg), diagnosed as psychalgia	Complete recovery
C.-M. Wu (Mrs.) 40, 4	Phobic neurosis, insomnia since 1995	Complete recovery in one half year

a: the column lists the name (sex), age, and number of years of practicing Zen-Buddhism.

b: glutamic-pyruvic transaminase (GPT≈20 for normal healthy people).

ECG, VEP, GSR, and EMG) recorded under the blessing power bestowed by the Zen master as well as under the normal Zen meditation. The surveys are analyzed by statistical analysis

Two wavelet-based algorithms, the Hurst exponent and the meditation-scenario interpreter using Fuzzy C-Means clustering, have been developed. The questionnaire survey study led to demonstration of the benefit of Zen meditation to the health. The meditation EEG analysis, on the other hand, revealed specific meditation scenarios and the inner light phenomenon as the unique finding that correlated particularly to the Zen meditation under spiritual blessing.



1.2 Survey of literature on the meditation research

Different meditating techniques have been studied for several decades. They are mostly the transcendental meditation (TM) [10]-[22], Yoga [23]-[26], Qi-Gong [27], Tibetan [28], and Japanese Zen meditation [29]-[30], with the focus mainly on the physiological and psychological effects of meditation. Numerous studies have focused on the physiological and psychological effects of meditation, with few addressing the underlying mechanisms. The search for physical and psychological correlates of meditation has centered essentially on three methods: Yoga in India, TM in the United States, and Zen Buddhism in Japan. Note that Zen Buddhism in Japan [30] was promulgated from mainland

China where orthodox Zen Buddhism originated.

In the study of psychological effect, researches mainly focus on the meditation effect on stress reduction, anxiety control, comprehensive capacity, and improvement of other mental activities and brain functions [31]-[34]. Meditation also improves the physiological conditions, such as moderation of hypertension, boost of immune function and endocrine secretion, even prevention of the cancer cells spreading [35]-[38].

During the past decades, the study of biomedical signals during meditation [39] has covered a wide scope including EEG, ECG [40], respiration [41], blood pressure, GSR, and fMRI (functional magnetic resonance image). This thesis is mainly devoted to the Zen meditation EEG. A number of papers have reported the EEG findings of subjects practicing various meditation techniques [42]-[48]. West [49] summarized those EEG findings and commented on the EEG changes during meditation as follows: On beginning meditation, an increase in alpha amplitude and a decrease in alpha frequency are often observed. Next, rhythmic theta trains may occur for experienced meditators. Thereafter and very rarely, bursts of high-frequency beta (above 20Hz) are recorded for meditators capable of achieving deep meditation, 'samadhi' or 'transcendence'. Thus, it was suggested that the pattern dominated by beta rhythm characterized the EEG of deep meditation stages.

Chapter 2 METHOD

2.1 Introduction of Biomedical signals

2.1.1 Introduction of EEG

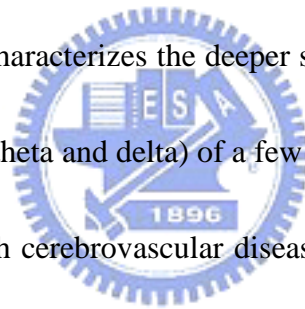
The electroencephalographic (EEG) signals, discovered in 1924 by Hans Berger [50], represent the tracings of summated cortical electrical activity collected by applying multiple recording sensors (called the "EEG electrodes") on the scalp (non-invasive recording) or on the cortex (invasive recording). The cortical potentials are actually the average of excitatory (EPSP) and inhibitory postsynaptic (IPSP) potentials from hundreds of neural cells nearby the recording electrodes [51]-[54]. After intensive research for several decades, the EEG has proved to be an important clinical tool for diagnosing and monitoring the central nervous system regarding normal or pathological conditions. For instance, sleep staging based on the EEG has been applied to the evaluation of sleep disorders [55]. Seizure detection and psychology state investigation are also important application for EEG [56]-[58].

The typical EEG signals are characterized by frequency, the rhythmic bands were classified as follows: delta band (1 ~ 4 Hz), theta band (4~ 8 Hz), alpha band (8 ~ 13 Hz), and beta band (13~ 25 Hz).

The most significant EEG rhythm when eyes open is beta wave. Beta wave is less than

20 μ V peak-to-peak over the entire brain. Beta wave occurs when eyes open or when one becomes alert. Occipital alpha dominates when an alert adult with eyes closed. Alpha rhythm is also associated with the relaxation state. It may be attenuated when eyes open or when one becomes alert.

In older children and young adults, bursts of 5Hz or 6Hz sinusoidal, bisynchronous, moderate-voltage theta may be seen in drowsiness or arousal anteriorly and temporally. Bursts of theta slowing may also occur during stage 2 sleep. The maximum voltage is usually central, that may be diffuse (anterior or posterior dominant). Increase of random, diffuse delta slowing normally characterizes the deeper stages of sleep for normal subjects. Note that temporal slow waves (theta and delta) of a few times the background amplitude in older subjects may correlate with cerebrovascular disease or with impairment of cognitive function.



In this study, the EEG signals were recorded from the scalp (non-invasive recording). The EEG electrodes are placed according to the definition of 10-20 system (see Figure 1). We can study the brain dynamics and spatial characteristics by analyzing the symmetrical behavior of frontal-versus-posterior or temporal electrodes.

In this thesis, we use EEGs to characterize the meditation stages and to interpret the meditation scenarios. Beside the common time-domain and frequency-domain analysis methods, we employed the time-frequency approach, mainly the wavelet decomposition, to

quantify the time-varying EEG spectral properties [59]-[66]. In addition, fuzzy clustering [67]-[73] was used to classify various EEG patterns. Hurst exponent [74] evaluated by wavelet method was modified for identifying a typical pattern correlating with an important meditation stage.

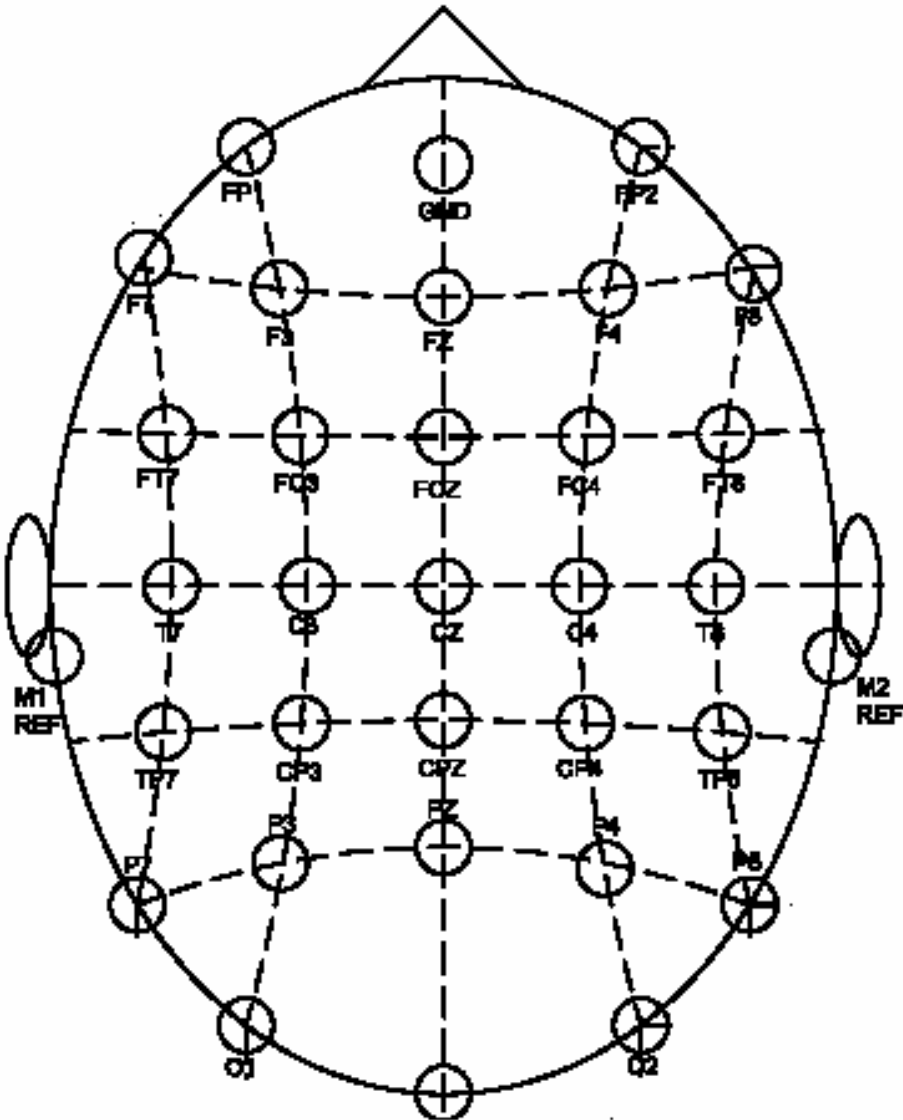


Figure 1 EEG electrodes displacement according to 10-20 system

2.1.2 Introduction of VEP

The visual evoked potential (VEP) is an evoked electrophysiological potential that can be extracted, using signal averaging, from the EEG activity recorded in the scalp. The VEP can provide important diagnostic information regarding the functional integrity of visual system [75]-[79].

Flash VEPs are variable across subjects than pattern responses but show little interocular asymmetry. They may be useful in patients who are unable or unwilling to cooperate for pattern VEPs, and when optical factors such as media opacities prevent the valid use for pattern stimuli. Due to the meditation practitioners must close their eyes during meditation; we use unpatterned flashes to get meditation VEP [80]-[81].

The visual evoked potential to flash stimulation consists of a series of negative and positive waves. The earliest detectable response has a peak latency of approximately 30 ms post-stimulus and components are recordable with peak latencies of up to 300 ms. Peaks are designated as negative and positive in a numerical sequence (see Figure 2). For the flash VEP, the most robust components are the N2 and P2 peaks. Measurements of P2 amplitude should be made from the positive P2 peak at around 120 ms to the preceding N2 peak at around 90 ms. In this paper, we compare the correlation between EEG and VEP to interpret the inner light effect during meditation.

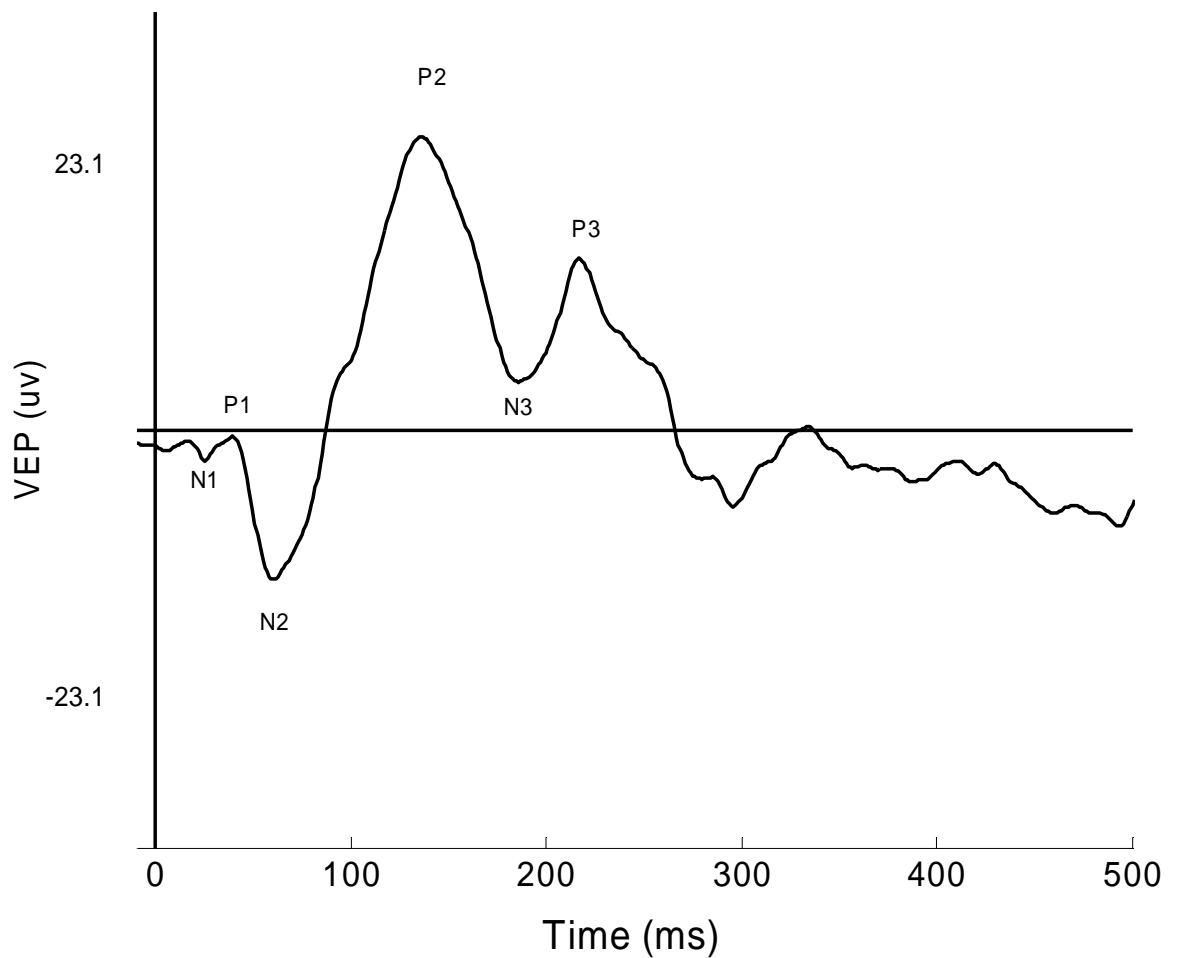


Figure 2 Typical VEP patterns.

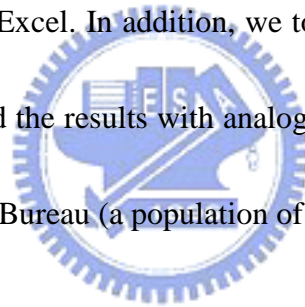
2.2 Data Recording Procedures

2.2.1 Health survey

Effects of practicing Zen-Buddhist meditation on the health promotion were analyzed according to the average number of using the Health Insurance Card. The questionnaires for this survey are shown in appendix-A. A total of 1,050 survey forms were distributed to the participants of a Zen-Buddhist meditation class. Twenty minutes were allotted for completing the forms. Afterwards, we retrieved 890 forms, of which 860 were correctly

filled as were requested. The results of statistical analysis presented in this paper are thus based on a bin of 860 cases with a wide range of ages (16~75 years). The mean age of the subjects is 40.2 years with a standard deviation (std) of 12.1. The male-to-female ratio is approximately 4:6. The age groups were evenly distributed.

72 percents of the experimental subjects had at least a college education, indicating the popularity of Zen-Buddhist meditation in this sector of the populace. This also allowed us to assume that the subjects were less likely to have misunderstood the questionnaire contents that strengthened the reliability of the survey. Information gathered from the questionnaires was analyzed by Excel. In addition, we took note of the frequency of usage of the Health Card and compared the results with analogous data of the non-Zen-practicing populace gathered by the Health Bureau (a population of 21,869,478 in 2002) [82].



2.2.2 Blessing

2.2.2.1 Hypotheses of blessing: circuit resonance

By seeking Zen, one is actually seeking the true energy of life. The only thing being promulgated in Zen-Buddhism is the truth, the wisdom, and the power of Zen in nature. Based on the essence of orthodox Zen Buddhism, we hypothesize that its pivotal technique of meditation can be comprehended via the resonance phenomenon.

In a series RLC electrical circuit, the input sinusoid is amplified the most when its

frequency equals the resonance frequency of the circuit. No resonance occurs in the physiological, mental, conscious, or subconscious states due to the existence of selfhood (ego). To be in resonance with the inner light, disciples of Zen-Buddhism spend years preparing themselves for the moment of resonance. One of the preparations, for instance, involves transcending physiological habituation. The first step is to switch the respiration habit from chest to abdominal respiration. Then by guarding some important apertures, the qi-energy starts penetrating, from the corpora quadrigemina (the Wisdom Chakra), through the pineal gland (Figure 3), bridging the energy passage between cerebellum and cerebrum. Gradually, the human life system enters a unique state in harmony with nature and the universe (called “the unification of heaven, earth, and human”). In this state, one becomes more and more egoless and liberated, that is, his body and mind are free (without attachment) even though the person is still involved in masses of worldly work.

According to the elucidation above, meditation in orthodox Zen-Buddhism follows a different quintessence compared with other meditating methodologies. It needs to be noted that this kind of energy or light differs from the qi energy. The qi energy is generated by exploiting the physical and mental capacity of the human life system. An experienced qigong master may generate spiritual qi energy by exploiting the latent capacity of the subconscious. On the other hand, the inner energy can be uncovered only when one transcends the physical, mental, and subconscious realm.

In the blessings experiment, EEG changes during blessings were investigated. Blessing in orthodox Zen Buddhism indicates a substantial benefaction from the master. A true master in orthodox Zen Buddhism is required to attain the Buddhahood Trinity— full attainment of Buddha’s three bodies, the emanation body (Nirmanakaya), the truth body (Dharmakaya), and the blessedness body (Sambhogakaya). With the true energy (light) of life in nature he is thus able to help disciples [5]-[6].

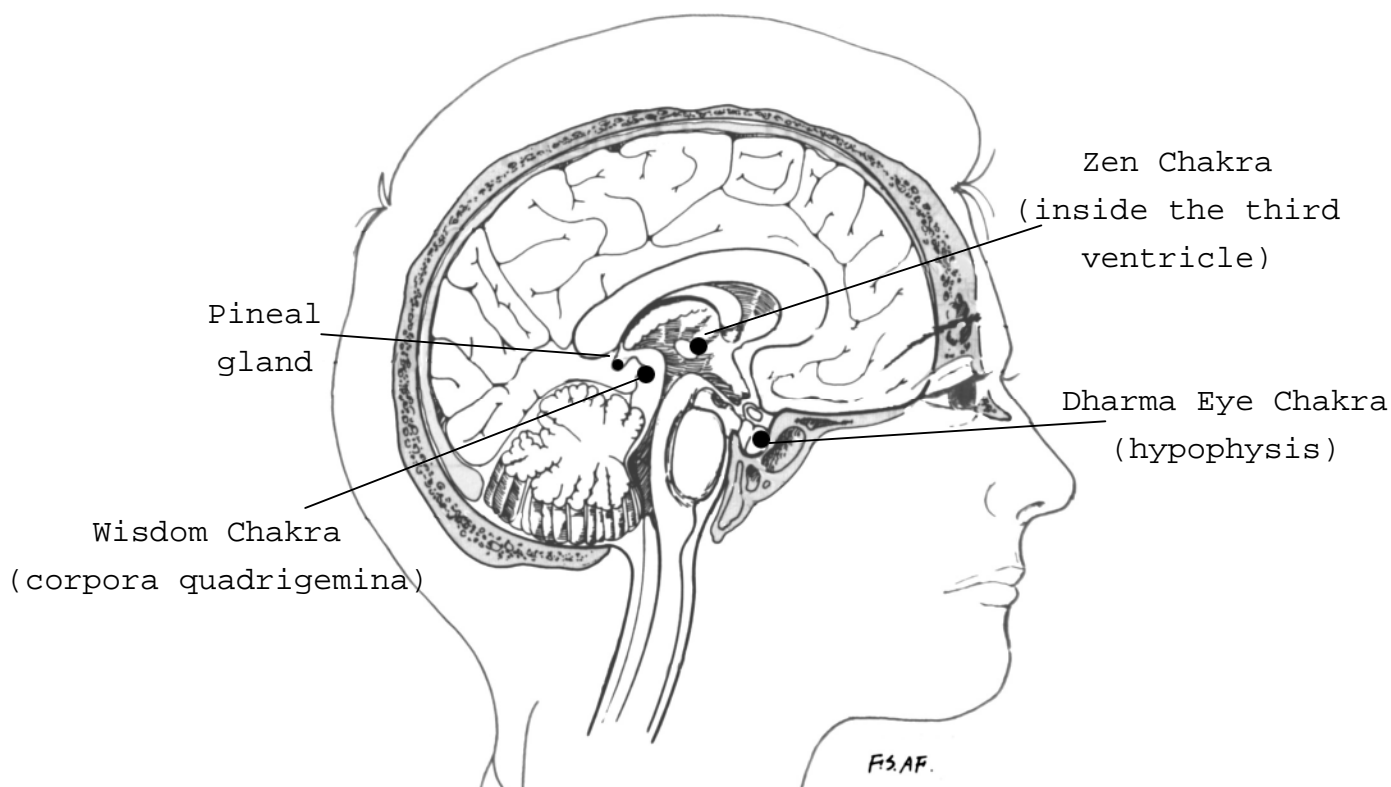


Figure 3 Some important apertures (Chakras) in Zen-Buddhist meditation.

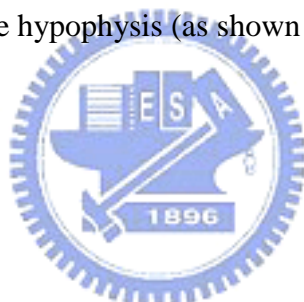
2.2.2.2 Experimental protocols of blessing

In our blessing experiment, master Wu Jue Miao Tian of the Zen-Buddhism Sect was invited to perform the blessing. A total of eight subjects were tested; among them, two subjects were non-meditators. Each subject was recorded twice, with one-week separation between the two recordings. The blessings ritual was performed in one recording only for each subject. It has been reported that blessings from master Wu Jue Miao Tian cured many people. To avoid the possibility of a placebo effect, the subjects did not know that they were to be blessed during the EEG recording. Master Wu Jue Miao Tian was not in the same room where the experiment was conducted. Both the experimental group (Zen-Buddhist practitioners) and the control group followed the same procedure: they were asked to sit, with eyes closed, in a normal relaxed position for 30 minutes. The blessings ritual, lasting for about 30 seconds, was provided once in each test. The effect of the blessing on the meditator normally continued till the end of meditation, as stated by the disciples in the post-experimental interview, although the blessing ritual itself lasted a short period. The effect of blessings on the EEG was compared between the experimental and control subjects.

2.2.3 Meditation EEG Scenarios

We applied the 8-channel unipolar recording montage of which the common reference was the linked MS1-MS2 (mastoid electrodes). The 8-channel EEG electrodes were placed

at F3, F4, C3, C4, P3, P4, O1, and O2. The sampling rate was 400Hz. Each recording lasted for 45 minutes, including the first 5-minute background EEG (the subject sat in normal relaxed position with eyes closed) and the rest 40-minute meditation EEG. During the meditation session, the subject sat, with eyes closed, in the full-lotus or half-lotus position. Each hand formed a special mudra (called the Grand Harmony Mudra), laid on the lap of the same side. The subject focused on the Zen Chakra and the Dharma Eye Chakra (also known as the “Third Eye Chakra”) in the beginning of meditation till transcending the physical and mental realm. The Zen Chakra locates inside the third ventricle, while the Dharma Eye Chakra locates at the hypophysis (as shown in Figure 3).



2.2.4 VEP

During the recording, subjects sat on a chair with eyes closed. The meditators practiced Zen-Buddhist meditation for 40 minutes. The control subjects just sat in a relaxation position for the same recording interval. Flash visual evoked potentials (F-VEPs) were recorded before, during and after meditation/relaxation, based on the 30-channel EEG montage (Figure 1). Each run consisted of 50 flash stimuli. The flash light was 10 us in duration and 2 Hz in frequency produced by a xenon lamp that was placed 60 cm in front of the subject's eyes.

2.3 Signal processing algorithms

2.3.1 Wavelet approach

For the past two decades, wavelet analysis has been extensively studied and proved to be a useful tool in biomedical signal processing [83]-[87]. Appropriate selection of scales and wavelet bases enables it to characterize the EEG rhythmic patterns [88]. The procedure is depicted below.

Firstly, the 2-second running window, moving at a step size of 1 second, is employed. And the entire meditation EEG record is divided into L segments. Consider a discrete-time signal $x[n]$, $0 \leq n \leq N-1$ ($N=800$), representing the l th running EEG epoch. The $a_j[n]$ and $d_j[n]$ indicate, respectively, the coarse and detailed sequences after j 's decompositions [89]-[90]. They can be obtained by

$$a_j[n] = \sum_{k=-\infty}^{\infty} a_{j-1}[k] \cdot h[2n-k], \text{ and} \quad (1)$$

$$d_j[n] = \sum_{k=-\infty}^{\infty} a_{j-1}[k] \cdot g[2n-k] \quad (2)$$

where $a_0[n] = x[n]$, the original EEG segment. According to the theory developed in multirate digital signal processing, $h[n]$ is the scaling filter, and $g[n]$ is the wavelet filter, the impulse responses $h[n]$ and $g[n]$ designed based on QMF (quadrature mirror filter) scheme relate to each other by:

$$h[n] = (-1)^{n+1} g[N - n + 1], n = 1 \dots N \quad (3)$$

where N is the length of $h[n]$.

The half-band filter coefficients of wavelet base db5 used in this study were

$$h[n] = [0.0033, -0.0126, -0.0062, 0.0776, -0.0322, -0.2423, 0.1384, 0.7243, 0.6038, 0.1601]$$

$$\text{and } g[n] = [-0.1601, 0.6038, -0.7243, 0.1384, 0.2423, -0.0322, -0.0776, -0.0062, 0.0126,$$

0.0033]. A wavelet base with a short filter length has a high temporal resolution; whereas

the wavelet bases with a long filter length has a high frequency resolution but also a higher

computational requirement. The db5 base was chosen in this paper as a good compromise

between decomposed EEG frequency resolution and computational requirements.

The l th running feature vector, $v_k[l]$, is extracted from the selected detailed-scale coefficients by computing their powers as

$$v_k[l] = \frac{1}{n_k} \sum_{i=1}^{n_k} d_k^2[i], \quad k = 4, 5, 6, 7 \quad (4)$$

where n_k is the length of d_k . The feature vector of the l th EEG epoch accordingly is

$$v[l] = \{v_4[l], v_5[l], v_6[l], v_7[l]\} \quad (5)$$

Finally,

$$\underline{V} = \{v[l] | 0 \leq l \leq L-1\}^T = \{v[0], \dots, v[L-1]\}^T \quad (6)$$

is an $L \times 4$ feature matrix of which each row indicates the running feature vectors.

In consideration of computational efficiency, the discrete Wavelet transform (DWT) is often applied. As illustrated in Table 2.1 and Figure 4, the DWT scales $D4 \sim D7$ are approximately matched to those well-defined EEG rhythmic bands, assuming a sampling rate of 400 Hz. The feature vector is thereafter constructed from these DWT coefficients.

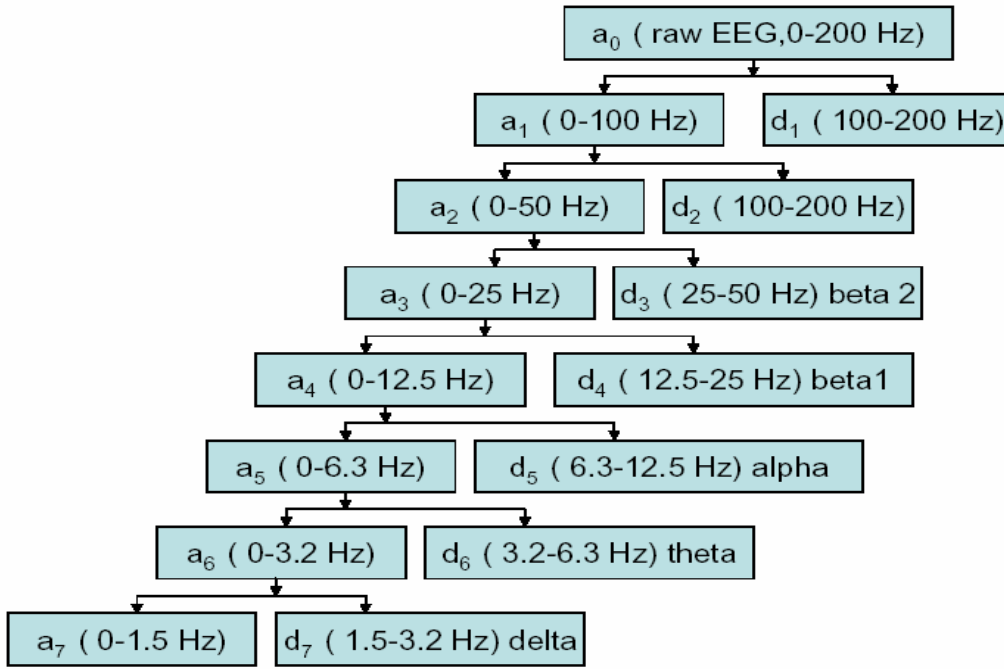


Figure 4 Illustration of wavelet decomposition of an EEG segment.

Table 2.1 EEG rhythmic bands and the corresponding wavelet filter frequency bands

(sampling rate $f_s=400\text{Hz}$).

EEG patterns	Δ (delta)	θ (theta)	α (alpha)	β (beta)
Rhythmic bands (Hz)	1~4 Hz	4~8 Hz	8~13 Hz	13~25 Hz
Wavelet detail component (D_i)	D7	D6	D5	D4
Frequency bands of (Hz) of D_i	1.5~3.1	3.1~6.2	6.2~12.5	12.5~25.0

2.3.2 Sub-Band Power

To illustrate the EEG evolution during the entire session, the percentage of wavelet sub-band power in each rhythmic band $p_j[l]$ was depicted by different shades of gray and calculated as followed:

$L \times 4$ sub-band power feature matrix \underline{V}' that is expressed by

$$\underline{V}' = \{v'[0], v'[1], \dots, v'[L - 1]\}^T, \quad (7)$$

where $v'[l]$ is the new (1×4) feature vector of the l th EEG epoch:

$$v'[l] = \{v'_4[l], v'_5[l], v'_6[l], v'_7[l]\}. \quad (8)$$

Elements in $v'[l]$ are derived from $v[l]$ in (4) and (5) by

$$v'_k[l] = \frac{v_k[l]}{v_t} \times 100 \%, \quad 4 \leq k \leq 7, \text{ where} \quad (9)$$

$$v_t = \sum_{k=4}^7 v_k[l] \quad (10)$$

The result was filtered twice by a low-pass, order 10, and moving average filters with impulse response $hs[n]$ to smooth the jiggling, where

$$hs[n] = \frac{\sum_{k=0}^{10} \delta[n-k]}{11} \quad (11)$$

Consequently, detailed variation was neglected.

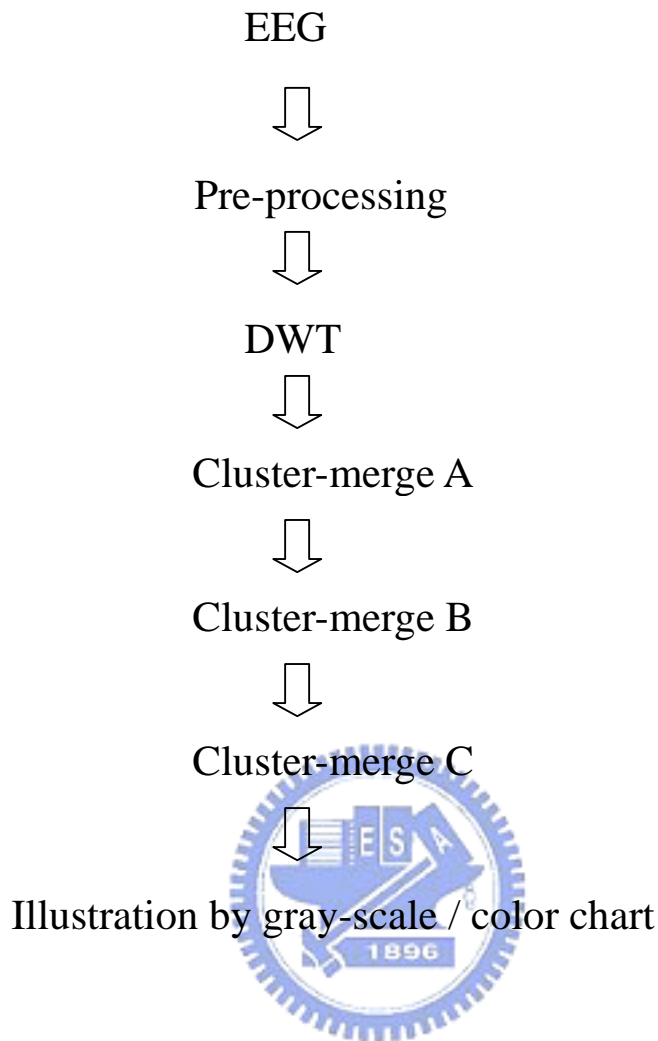


Figure 5(a) Block diagram of FCM-merging strategies, the flowchart of cluster-merge A~C are illustrated in Figure 5(b)~(d).

2.3.3 FCM clustering

Automatic interpretation algorithm often involves three strategies: (1) derivation of feature basis, (2) feature clustering, and (3) scoring (interpretation) based on the feature clusters [91]-[93]. Feature extraction aims at transforming the input data into a form (feature vector) appropriate for the clustering algorithm to identify the clusters. The feature

vector in this study is derived from wavelet coefficients. Each feature vector, after processed by the FCM, introduced by Bezdek JC, belongs to a cluster to some degree that is specified by a membership matrix [94]. According to our experience in EEG feature classification, conventional FCM algorithm, without the background knowledge of EEG characteristics, cannot effectively classify and interpret the EEG record in comparison with the naked-eye examination. We thus developed a novel approach, with three cluster-merging strategies, for the meditation EEG analysis. The main attribute is its knowledge-based processing of EEG record that is encoded into an easily comprehensible chart of meditation scenario. Figure 5(a) illustrates the overall strategy developed according to our experiences on meditation EEG characteristics. The FCM-merging strategies involving three cluster-merging subroutines (Figure 5(b), 5(c), and 5(d)) are designed particularly to solve the problem of blind clustering by simple FCM algorithm. Cluster-merge A (Figure 5(b)) mainly determines the number of clusters (K) by the criterion of cluster-center distance (D_{ij}). Note that the number of clusters is often initialized to be larger than that required. Further processing of clusters thus does not involve splitting. Cluster-merge B (Figure 5(c)) eliminates those clusters characterizing transient activities. Finally, cluster-merge C (Figure 5(d)) assigns different clusters, actually representing the same EEG rhythm with amplitude fluctuation, to be the same one. We first describe the FCM function in subroutines cluster-merge A and B. The FCM function analyzes the EEG data and produces three outputs: (1) the membership matrix \underline{U} , (2) the cluster centers $\{c_i$,

$i=1, \dots, K\}$, and (3) the EEG coding vector (row matrix) \underline{S} . Four steps in the FCM function are depicted below.

Step 1: Initialize the membership matrix \underline{U} with random values between 0 and 1. The size of \underline{U} is $K \times L$, where K is number of clusters, and L is the number of input feature vectors. The element of membership matrix \underline{U} , u_{ij} , is the probability that the j th feature vector belongs to the i th cluster ($1 \leq i \leq K$ and $0 \leq j \leq L-1$). Note that, for a given feature vector, summation of degrees of belongness equals unity. Elements of \underline{U} must satisfy the constraint below

$$\sum_{i=1}^K u_{ij} = 1, \quad 0 \leq j \leq L-1. \quad (12)$$

Step 2: Calculate fuzzy cluster centers for all K clusters according to

$$c_i = \frac{\sum_{j=0}^{L-1} v[j] \cdot u_{ij}}{\sum_{j=0}^{L-1} u_{ij}}, \quad 1 \leq i \leq K, \quad (13)$$

where $v[j]$ is the feature vector (1×4 row vector) derived from wavelet coefficients defined in equation (5).

Step 3: Compute the cost function defined below

$$J(\underline{U}, c_1, c_2, \dots, c_K) = \sum_{i=1}^K J_i = \sum_{i=1}^K \sum_{j=0}^{L-1} u_{ij}^m D_{ij}^2, \quad (14)$$

$$\text{where } D_{ij} = \|c_i - v[j]\| \quad (15)$$

is the Euclidean distance between the i th cluster center and the j th feature vector.

The weighting exponent, m , in (14) is selected to be $m=2$. The criterion requires J to be as small as possible. The iteration terminates if improvement of J over previous iteration is below a pre-specified threshold. Otherwise, the algorithm proceeds with next step to update the membership matrix \underline{U} .

Step 4: Compute a new membership matrix \underline{U} whose element u_{ij} is adjusted by

$$u_{ij} = \frac{1}{\sum_{k=1}^K \left(\frac{D_{ij}}{D_{kj}} \right)^{\frac{2}{m-1}}}, \quad 1 \leq i \leq K, \quad 0 \leq j \leq L-1. \quad (16)$$

According to the above equation, u_{ij} is inversely proportional to the squared distance from the feature $v[j]$ to the cluster center c_i .

The iteration process from *Step 2* to *Step 4* continues.



2.3.4 FCM-merging strategies

The FCM function described above blindly classifies the EEG patterns based on quantitative features. Consequently, the result of interpretation often appears to be away from satisfaction. We accordingly developed sophisticated cluster-managing strategies, the FCM-merging strategies, based on background knowledge of meditation EEG characteristics, for achieving an interpretation closer to the result of naked-eye examination. We first generate a $1 \times L$ long-code row vector matrix, $\underline{\mathbf{S}} = \{s_j, 0 \leq j \leq L-1\}$, representing the encoded stream of L feature vectors. Each element ($s_j \in \text{integer}$) indicates, among K clusters,

the particular cluster to which the j th feature vector belongs, $1 \leq s_j \leq K$. It is determined by finding the row index i (denoted by s_j) such that $u_{s_j j} = \max_i \{u_{ij}\}$, $1 \leq i \leq K$, considering the j th feature vector.

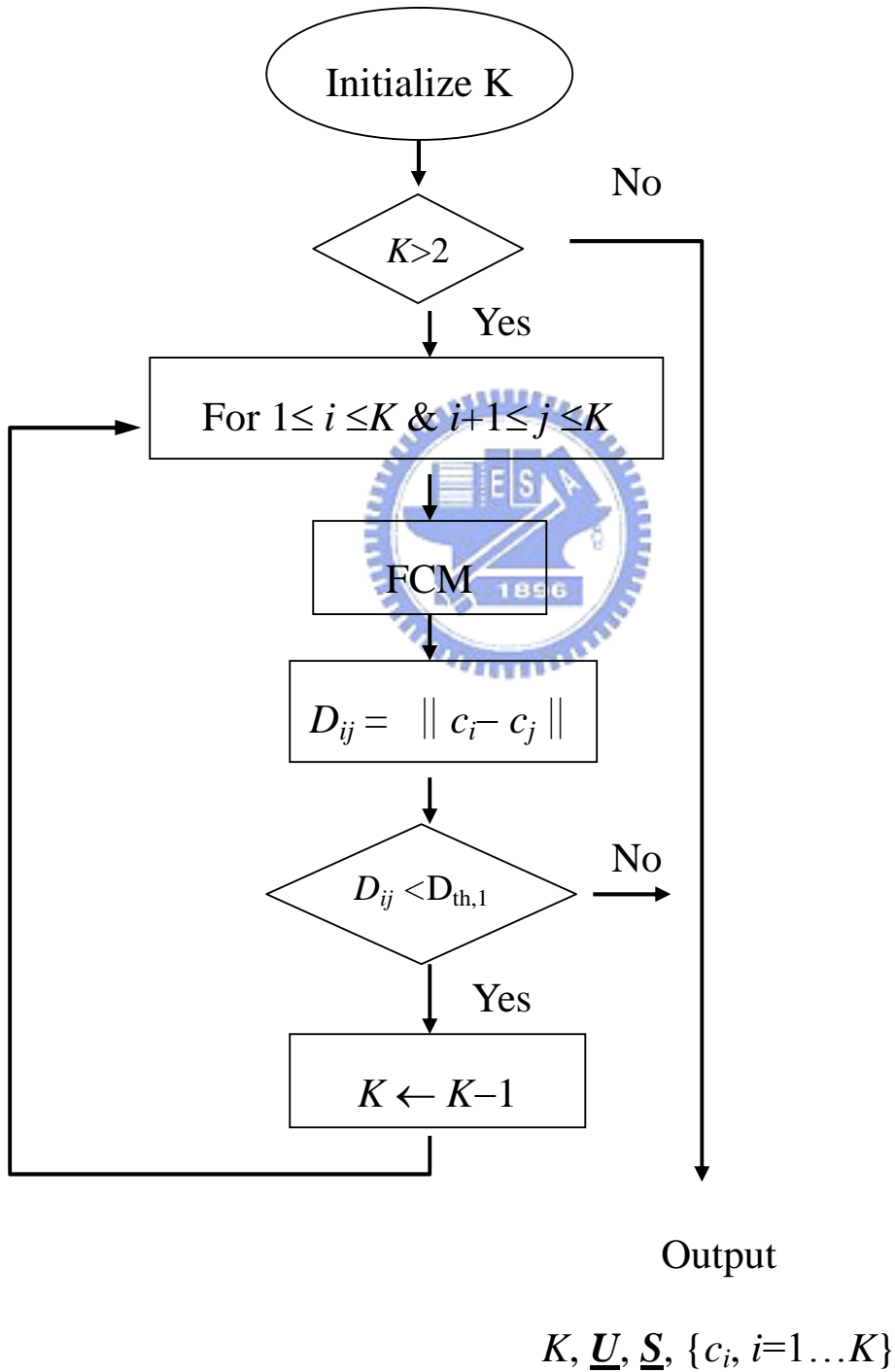
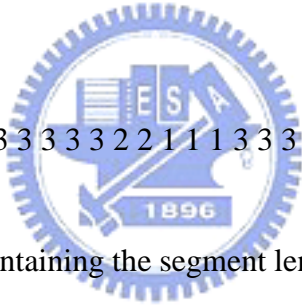


Figure 5(b) Flowchart of cluster-merge A

In the cluster-merge A subroutine (Figure 5(b)), number of clusters (K) is justified by having the inter-distance between cluster centers (D_{ij}) no less than a pre-specified threshold $D_{th,1}$. Four outputs available are: number of clusters (K), membership matrix (\underline{U}), EEG coding vector (\underline{S}), and the cluster centers $\{c_i, 1 \leq i \leq K\}$, of which only K and \underline{S} feed into the *cluster-merge* B subroutine (Figure 5(c)). Based on the coding vector \underline{S} , cluster-merge B first analyzes the maximum length of code- k feature ($1 \leq k \leq K$), $\max-l_{sk}$. The length of code- k feature (l_{sk}) denotes the number of consecutive code k 's. Consider an example of three clusters ($K=3$) obtained by analyzing 18 feature vectors ($L=18$). Assume the coding vector generated by cluster-merge A is:



$$\underline{S} = \{1 \ 1 \ 3 \ 3 \ 3 \ 3 \ 3 \ 2 \ 2 \ 1 \ 1 \ 1 \ 3 \ 3 \ 3 \ 3 \ 2 \ 2\}, \quad (17)$$

we then obtain three sets, each containing the segment lengths of code- k feature ($1 \leq k \leq 3$):

$$\underline{l}_{s1} = \{2 \ 3\}, \underline{l}_{s2} = \{2 \ 2\}, \underline{l}_{s3} = \{5 \ 4\}. \quad (18)$$

All the numbers in the K sets are accordingly summed up to be L . From (18), the maximum length of code- k feature is: $\max-l_{s1}=3$, $\max-l_{s2}=2$, and $\max-l_{s3}=5$. If $D_{th,2}=3$, cluster-merge B subroutine will decrease K by 1 since $\min_k \{\max-l_{sk}\}=2 < D_{th,2}$. Otherwise, the last merging subroutine follows. After the operation of cluster-merge B, the value of K is more substantial and practical. The coding vector \underline{S} is then derived using the final K 's, and both are fed into cluster-merge C subroutine. The goal of cluster-merge B is to eliminate the tedious work of interpreting those insignificant transient activities, which tend to

complicate the result.

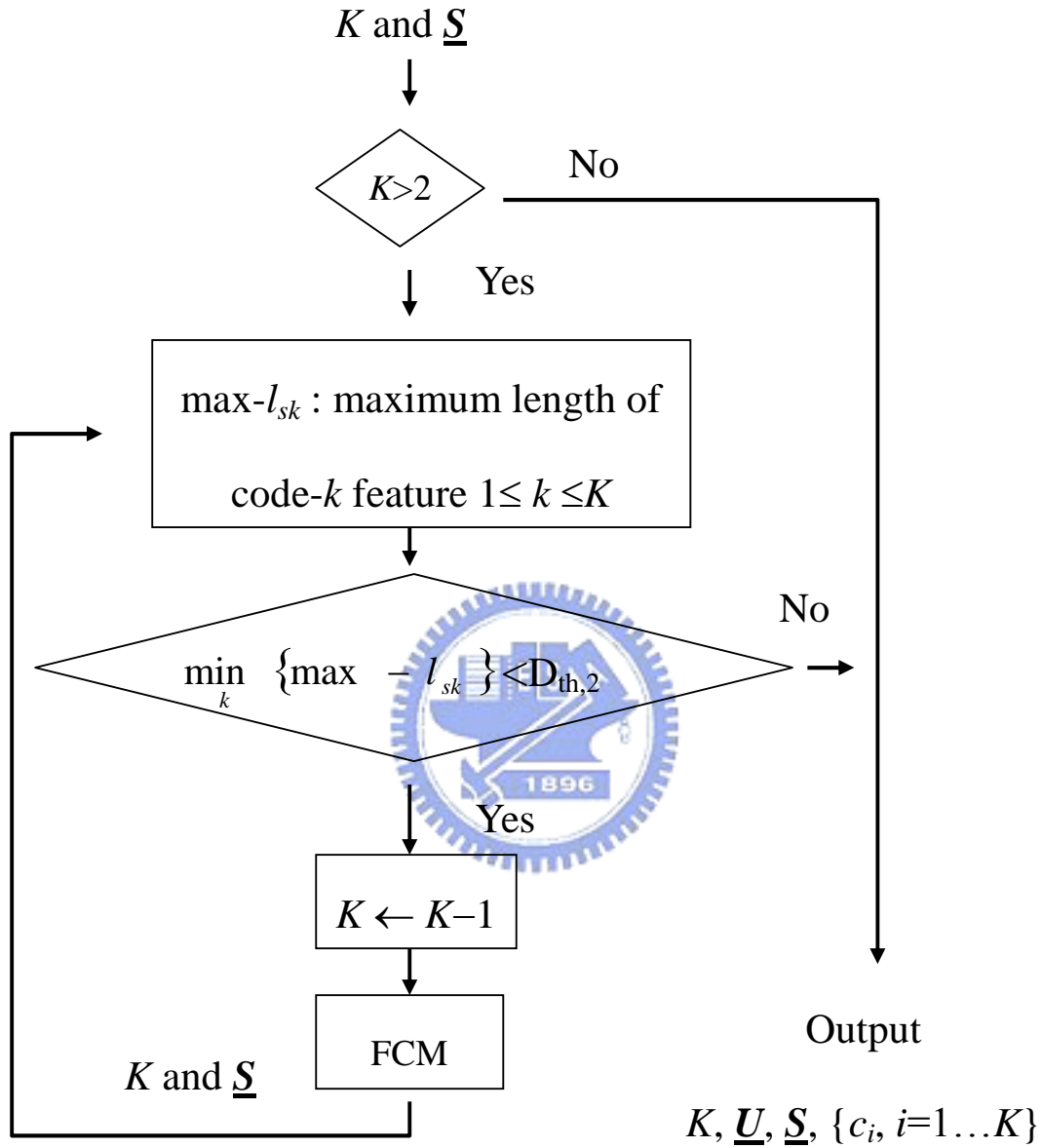


Figure 5(c) Flowchart of cluster-merge B

In EEG, considerable variation in amplitude often obscures identification of certain rhythmic pattern. For instance, FCM function tends to output multiple clusters for α rhythm classified according to the squared wavelet coefficients. This situation also occurs to Δ and

θ rhythms. Cluster-merge C subroutine hence reexamines and corrects the fault by computing the subband power ratios according to equation (7)~(10). Based on the modified feature matrix \underline{V}' , FCM function outputs a set of new cluster centers $\{c'_i, 1 \leq i \leq K\}$. If cluster j has a center c'_j close enough to the center of cluster i (i.e., $D'_{ij} = \|c'_i - c'_j\| < D_{th,3}$), the coding vector \underline{S} (output of cluster-merge B) will be modified by re-encoding cluster j as cluster i . In this way, different clusters actually containing feature vectors of the same EEG rhythm (e.g., α or θ) are to be identified and interpreted as the same one via an adequate choice of $D_{th,3}$. It is noted that if the sub-band power ratios are employed in the very beginning (*cluster-merge A*), clustering performance is incorrigibly poor due to failure in separating different EEG rhythms. That is, cluster-merge C does not innovate upon the coding vector \underline{S} . Instead, it re-indexes those clusters, all referred to the same EEG rhythm, by the same code.

In meditation EEG study, the range $2 \leq K \leq 5$ is a moderate selection according to our experience in meditation EEG interpretation. However, there always exists inter-subject variation in biomedical signals. Our algorithm thus begins with a large value of K (normally, $K=9$) and, through the cluster-merging subroutines succeeded, further refines the interpreting results.

The FCM-merging strategies, systematically and effectively encoding the quantitative EEG features, were also proven to be robust to implementing parameters. Moreover, a wide

range of mother wavelet prototypes can be used without changing the interpreting result should the wavelet duration be long enough. For instance, mother wavelets like the db3, db5, db10, sym3, and sym5 generated by MATLAB result in the same interpretation although the feature vectors derived midway are slightly different. We thus employed the mother wavelet db5 in consideration of computational efficiency.

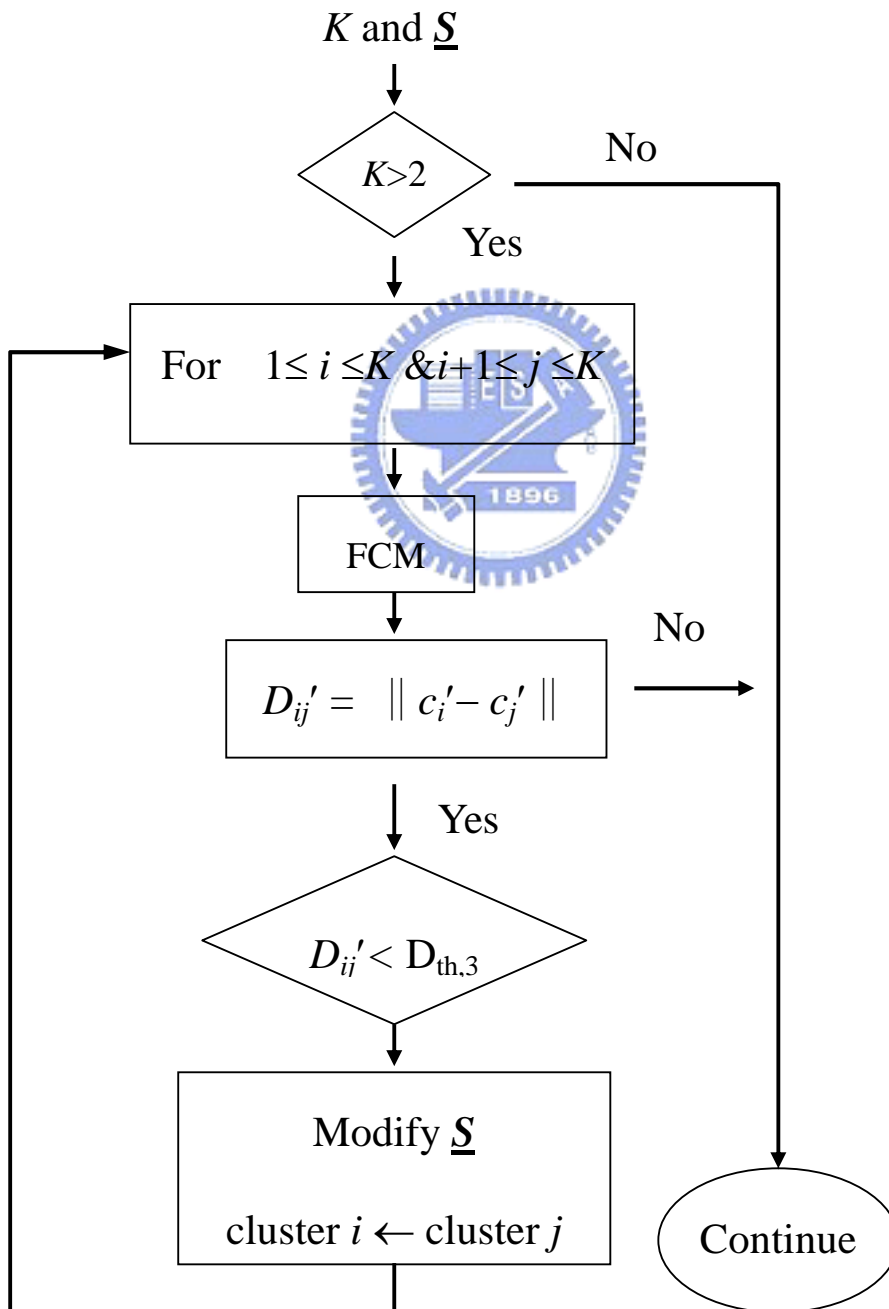


Figure 5(d) Flowchart of cluster-merge C

2.3.5 Hurst exponent

The features of beta rhythm are relatively small using time-domain and frequency-domain analyses. Beta rhythm is a low-amplitude wave with higher frequency contents compared to other EEG rhythms, and is often embedded in other higher amplitude rhythms such as alpha rhythms. Some beta rhythms are often misclassified as base-line drifts and low-amplitude alpha rhythms when using the quantitative features derived from the normal time- and frequency-domain analyzing methods.

This section described a novel algorithm for identifying beta rhythms. Two major strategies of the algorithm are: (1) EEG feature extraction based on estimate of the Hurst exponent, H , and (2) computation of the linear-regression line fitting error. The Hurst exponent, H , is the parameter of fractional Brownian motion (fBM) modeling the $1/f$ process. Some papers have already discussed the possibility of applying H to the biomedical signals to extract particular features and to detect specified components [95]. However, to the best of our knowledge, the application of H to EEG data has never been examined. Wornell and Oppenheim proposed a method to estimate H via wavelet-decomposed coefficients, which makes the calculation of H more straightforward and efficient [96]-[97].

The proposed method, H-SSE based algorithm, estimates H and the regression fitting error (SSE: the sum of square errors of interpolation) of each EEG segment which are used as the quantitative features for interpreting the EEG record. The H-SSE based algorithm

nonlinearly rescales the EEG rhythms to magnify the feature space of beta rhythms that has been infeasible in the time-domain and frequency-domain analyses. In addition, the algorithm is capable of distinguishing low-amplitude alpha and beta rhythms from complex EEG segments with vaguely defined patterns. The procedures are as following:

At first we extract EEG wavelet features as equation (1) to equation (3). Then take the logarithms of variance of the detailed-part coefficients,

$$y_j = \log_2(\text{var}(d_j[n])), j=4-7, \quad (19)$$

As shown in Figure 6, the slope (ρ_d) of the linear regression line fitting the y_j -versus- j data points provides an estimate of H; that is,

$$\rho_d = 2H + 1 \quad (20)$$



Finally, SSE is evaluated below

$$\text{SSE} = \sum_{j=4}^7 (y_j - \hat{y}_j)^2, \quad (21)$$

where \hat{y}_j is the interpolation point on the regression line.

The window length is also 2 seconds with a moving step of one second for the consecutive, long-term EEG analysis. From the definition of H and SSE, we expect that EEG theta and alpha rhythms would have higher regression errors, and result in a higher SSE value for the corresponding wavelet scale levels 6 and 5 that are located in the middle region of the regression line; whereas delta and beta rhythms have a lower SSE and the

opposite sign of H.

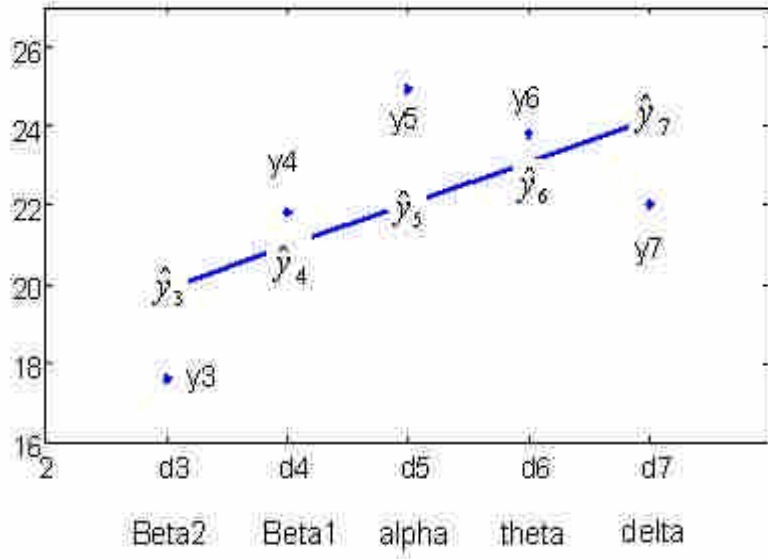


Figure 6 Chart of H&SSE pairs calculation.

2.3.6 Alpha-suppressed EEG identification

The powers of detail component of the scale ranging from 5 to 8 correspond to the beta, alpha, theta, and delta for sampling rate 1000 Hz EEG is similar to equation (4)

$$v_k[l] = \frac{1}{n_k} \sum_{i=1}^{n_k} d_k^2[i], \quad k = 4,5,6,7 \quad (22)$$

To be qualified as an alpha-suppressed EEG component, four power values are required to be smaller than $\theta_k, k = 5,6,7,8$, the pre-determined threshold values of v_k . Let $Low[l]$

encode the state of alpha in a given segment, and

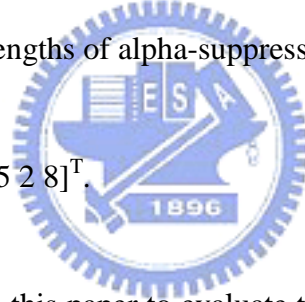
$$Low [l] = 1, \text{ when } v_k[l] < \theta_k, k = 5,6,7,8, \text{ otherwise } Low [l] = 0 . \quad (23)$$

The segment length code \underline{S} of alpha-suppressed EEG Low can be calculated as the following example. Given

$$Low = [0 0 1 1 1 1 0 1 1 1 1 1 0 1 1 0 1 1 1 1 1 1 1 1] ^T, \quad (24)$$

we then have four alpha-suppressed segments of lengths 4, 5, 2, and 8 (in number of epochs, in this case that is also in number of seconds). Let vector \underline{S} be the row matrix of which the elements are the corresponding lengths of alpha-suppressed segments identified. It becomes

$$\underline{S} = [4 5 2 8] ^T. \quad (25)$$



Two parameters are defined in this paper to evaluate the significance of low-power EEG contents [19]; one is the total length of low-power EEG segments

$$S_{total} = \sum_{i=1}^{ls} \underline{S}[i], \text{ where } ls \text{ is the length of } S, \quad (26)$$

and the other is the maximum length of the continuous alpha-suppressed EEG segments in each single subject

$$S_{max} = \max\{\underline{S}\}, \quad (27)$$

For the example illustrated above, $S_{max}=8$. Accordingly, two quantities (S_{total} and S_{max}) are

used to characterize the alpha-suppressed EEG for one subject.

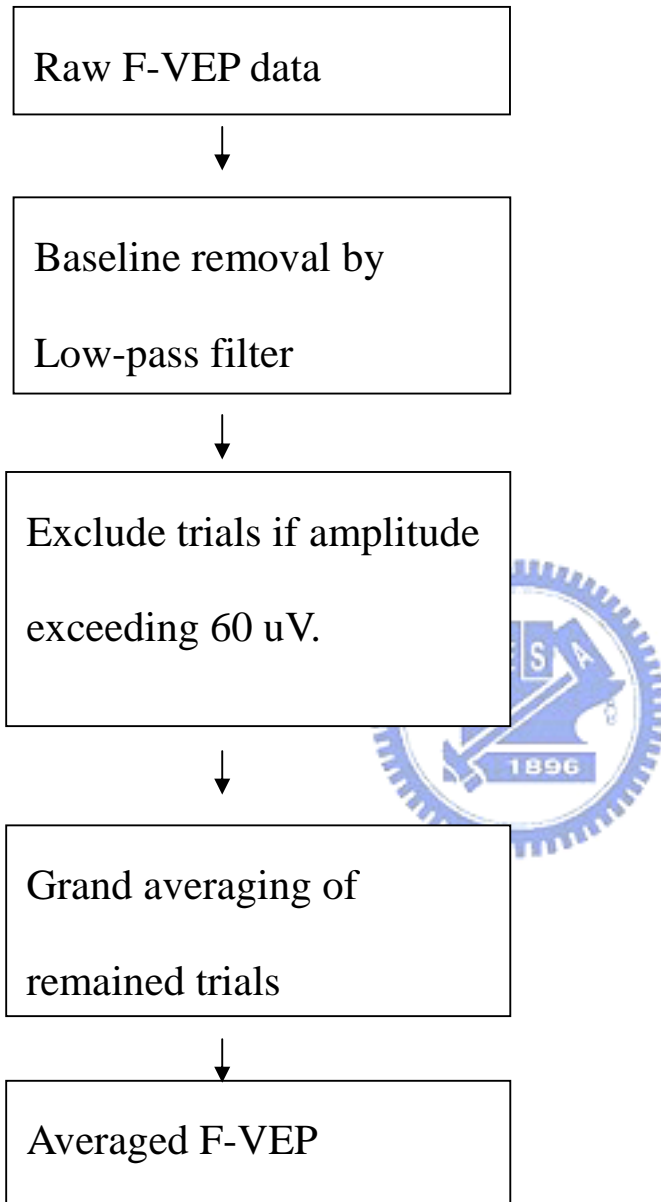


Figure 7 F-VEP preprocessing algorithms

2.3.7 VEP waveform feature extraction

Firstly, each raw trial was baseline-calibrated by subtracting the value computed from

the average of the 200 ms interval before stimulus onset. Furthermore, trials with absolute peaks > 60 uV were excluded. The F-VEP was estimated by averaging total 50 trials, which had been preprocessed by previous procedure. Figure 7 illustrates the F-VEP preprocessing algorithms.

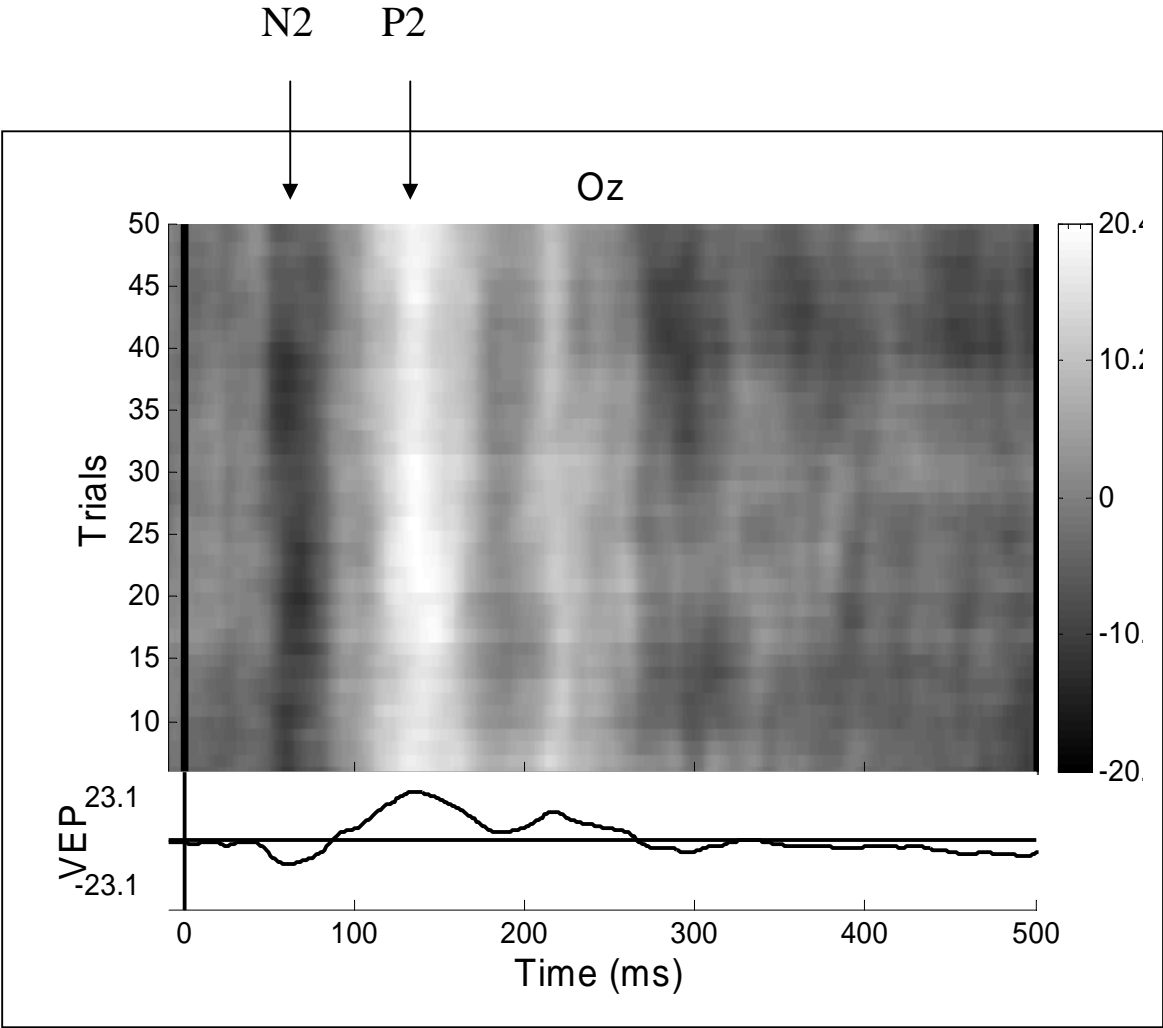


Figure 8 demonstrates the F-VEP map

Figure 8 demonstrates the F-VEP map made by stacking all the trials and transforming the F-VEP magnitudes into gray intensities for 2D grayscale image display. The bottom of Figure 8 is the averaged F-VEP pattern (Figure 8 was implemented by the software EEGLAB developed by Delorme A and Makeig S [100]). This map reveals that N2 and P2 are the most significant peaks in each trial.




Chapter 3 RESULTS

3.1 Health Survey

3.1.1 Experiences of Zen practitioners.

In the bin surveyed, the mean length of Zen-Buddhist practice is 7.1 years (std=5.4).

The histogram of practicing length (number of years) appears to be an evenly distributed statistics in the experimental group. The average practicing frequency is 5.3 times (std=3.7) per week.



Note that, when practicing Zen-Buddhist meditation, the practitioners may sit in the full-lotus, the half-lotus, or the free-style position. In the bin of 860 experimental subjects, the distribution of the possible meditation durations is summarized in Table 3.1 for each meditation position. The possible meditation duration refers to the estimated length of each meditation session. The weekly practicing frequency and the number of practicing years are shown under the value of meditation duration, as a reference, for different meditation positions. A larger range of deviation is observed for the group of free-style meditation that is found consisting of practitioners with less experience. In other words, the accumulation of meditation experience improves the flexibility of muscles and bones so that more practitioners can meditate in the full-lotus position. In Table 3.1, the weekly meditation

frequency reflects the diligent habit of Zen meditation. Apparently, regularity and frequency have significant effect on the improvement of meditation posture.

Table 3.1 Distribution of the meditation lengths for each meditation position from survey result.

Meditation position		Full-lotus	Half-lotus	Free-style
Number of practitioners		306 (35.6%)	508 (59.0%)	46 (5.4%)
Meditation length mean±std (minute)	Male	59.2±19.0 5.5weekly, 7.2yr	55.1±18.1 5.0weekly, 6.9yr	50.8±36.4 3.5weekly, 4.9yr
	Female	53.7±15.3 5.7weekly, 7.4yr	52.4±19.8 5.2weekly, 6.8yr	42.6±18.3 4.0weekly, 6.1yr
	Overall	56.5±17.5	53.3±19.3	46.1±27.4

We also surveyed the frequency of smoking and drinking alcohol among the 860 experimental subjects. Only 10.5 percent of the subjects are smokers, yet, half of them smoke infrequently. This rate is significant lower than that of the smoking population in Taiwan (male: 39.2 percent, female: 3.3 percent). Respecting the drinking survey, 66.8 percent have never drunk since their Zen-Buddhist practice, and 24.9 percent seldom drink.

Only approximately 4 percent of the subjects have the lifestyle of regular drinking. According to our survey, more than 8 percent of the populations in Taiwan have the problem of alcohol abuse. As a consequence, Zen-Buddhist practice leads to a much healthier lifestyle. As a matter of fact, it has been reported that meditators achieved the following biological reactions: marked reduction in oxygen use, notably lower secretion of stress hormones, increase in immune factors, reduction of anxiety, reduction of chronic pain, etc [4]. The report might provide a strong reasoning for our results of healthy living habits among meditation practitioners.



3.1.2 Psychological and mental health of the experimental subjects.

Table 3.2 depicts the results of the everyday condition of the frame of mind, according to the self evaluation by the 860 experimental subjects. Note that the value of grade ranging from 1 to 5 scores the condition varying from the worst to the best, with the mid-value (grade=3) indicating the normal, average condition. In other words, better mental health is quantified by a higher grade for all the cases. More than 90 percent of the practitioners feel content and happy in their daily lives. Less than 20 percent feel the life stress. Most practitioners (~90 percent) are well capable of moderating the occasional stresses (grade=4 and 5).

Table 3.2 Survey results of self evaluation of the daily frame of mind (experimental subjects). Grade ranging from 1 to 5 indicates the condition varying from the worst to the best.

grade item	1	2	3	4	5
Contentment (1 year ago)	0.1%	0.6%	11.9%	25.4%	62.0%
Contentment (currently)	0.3%	0.7%	8.5%	39.1%	51.4%
Feeling of stress	5.4%	13.8%	14.2%	46.1%	20.6%
Ability of moderating stress	0.0%	2.2%	8.5%	48.9%	40.4%



We further examine the effect of weekly practicing frequency and total practicing years on the mental health. Figure 9 illustrates the histogram of contentment and stress moderation on the weekly practicing frequency (number of times) that, obviously, demonstrates a positive correlation between the mental health and the practicing frequency. Similar trend is observed in the histogram of Figure 10 based on the number of practicing years. Nevertheless, we found that, to be totally released from the feeling of daily-life stress, most practitioner spent more than seven years in the intense and highly devoted Zen-Buddhist practice. As addressed in the Diamond Sutra [98], to disclose the enlightened wisdom, a Zen-Buddhist disciple should be detached, that is, without regard to appearances, without regard to sound, odor, touch, mind and mood... without any attachment.

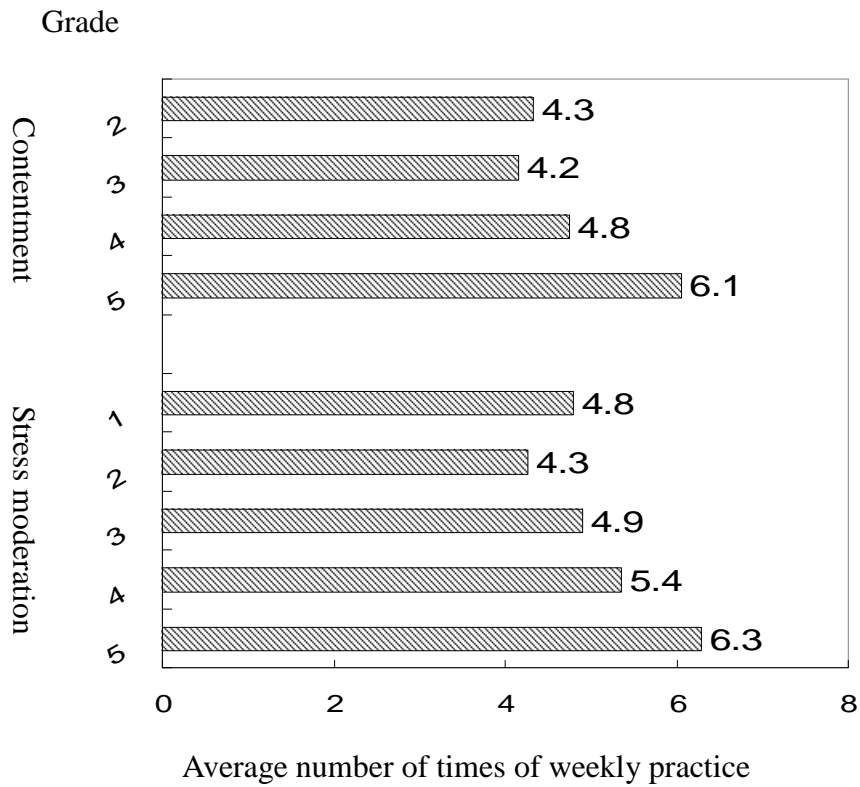


Figure 9 Histogram of contentment and stress moderation on the weekly practicing frequency (number of times).

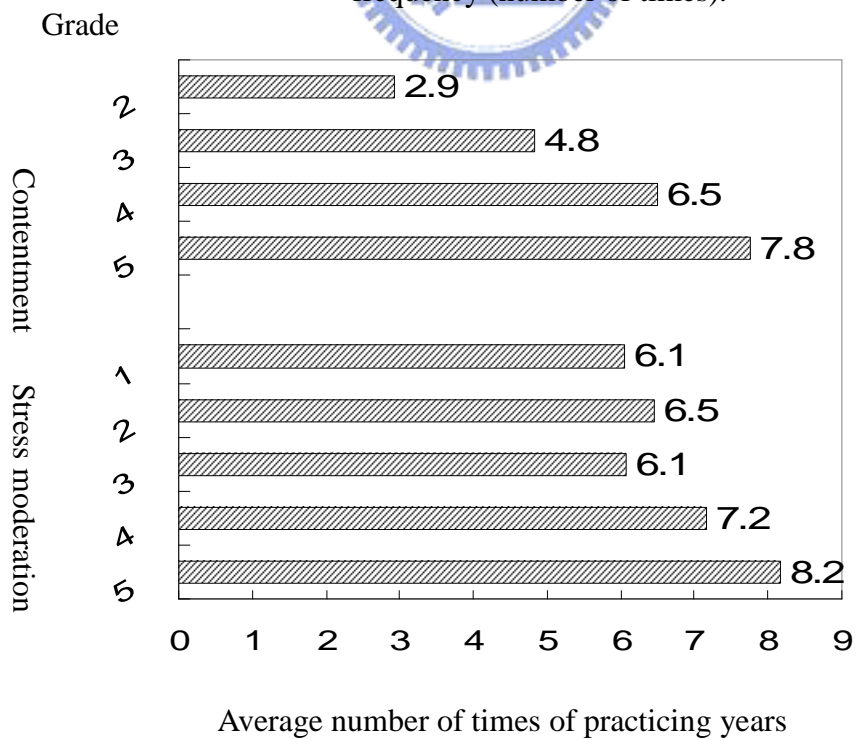


Figure 10 Histogram of contentment and stress moderation on the practicing years.

Figure 11 displays the histogram $h(s_g)=n_g$, where $1 \leq s_g \leq 5$ denotes the grade of ability of moderating the stress feeling, and n_g is the number of experimental subjects who are in the group of stress-moderation grade = s_g . Different gray-colored bars are used to illustrate the histogram of a group who practice the Zen-Buddhist meditation in a similar weekly frequency. For example, the white-colored (black-colored) bar illustrates the number of subjects that practice 1-3 (>7) times per week. It appears that the practicing frequency does little good to help the stress problem. On the other hand, as shown in Figure 12, length of meditation practice shows significant impact on improving the stress-moderation ability. Similar phenomenon is observed in Figures 13 and Figure 14, demonstrating the effect of weekly practicing frequency and practicing length (in number of years) on the grade of contentment.

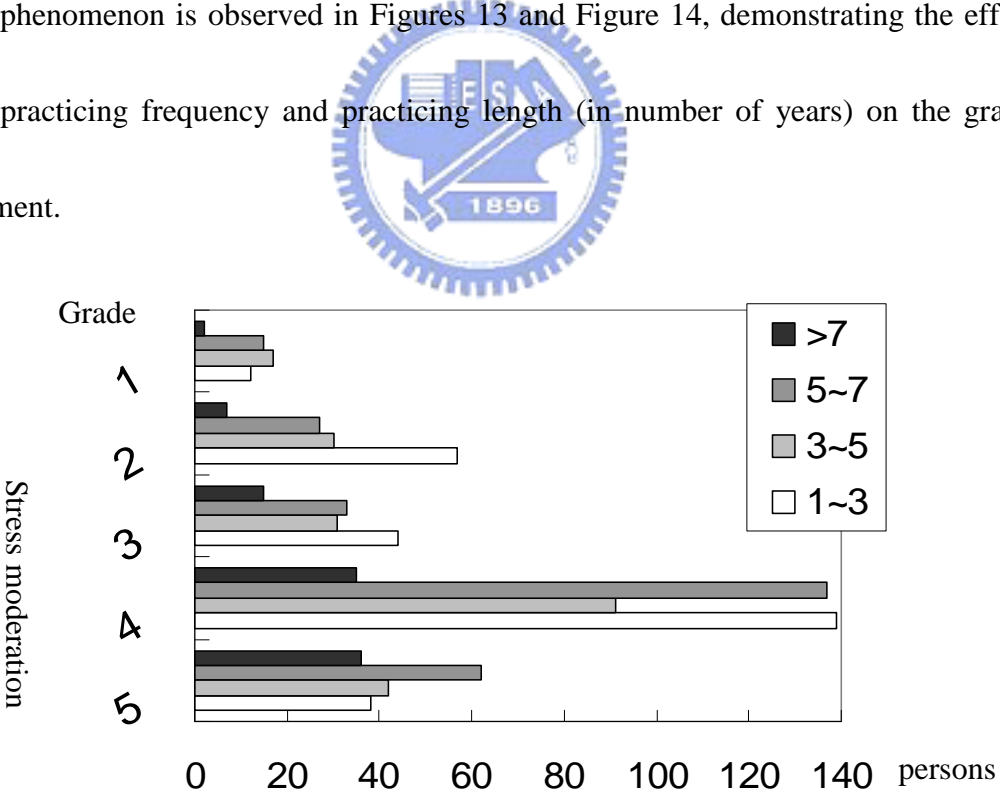


Figure 11 Histogram of stress moderation on the number of experimental subjects under the same stress moderation grade. Different bar colors are used to identify various weekly practicing frequencies

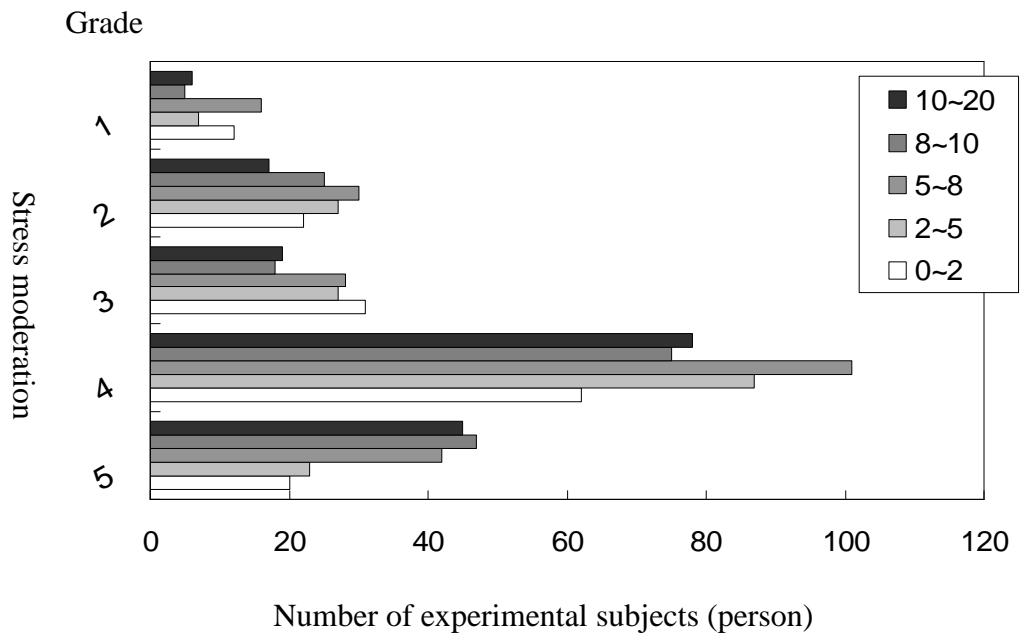


Figure 12 Histogram of stress moderation: distribution of the number of experimental subjects under the same stress moderation grade. Different bar colors are used to identify various lengths of meditation experiences (in number of years).

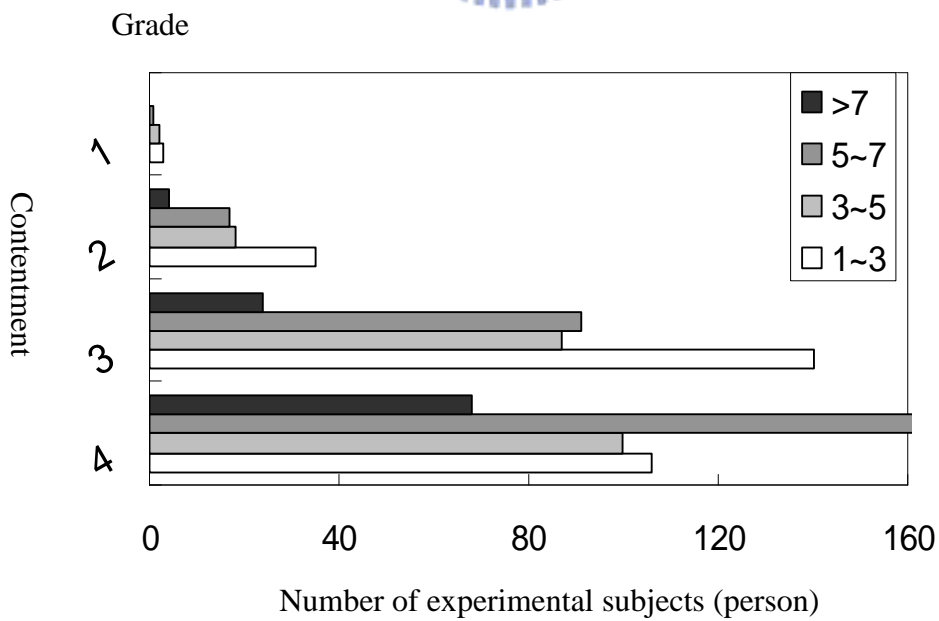


Figure 13 Histogram of contentment of various weekly practicing frequencies.

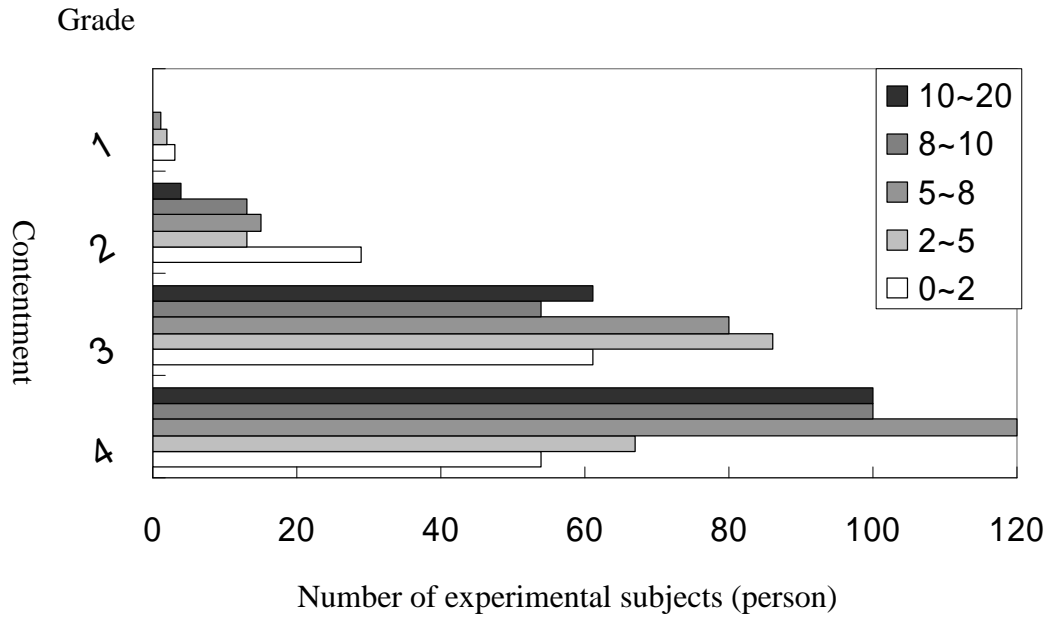


Figure 14 Histogram of contentment: distribution of the number of experimental subjects

under the same contentment grade. Different bar colors are used to identify various lengths of meditation experiences (in number of years).



3.1.3 Physiological health conditions in the experimental group.

According to the 2002 statistical data provided by the Bureau of National Health Insurance in Taiwan [82], the average number of outpatient services requested by each person was 14.52 based on population 21,869,478 and that was 4.6 for the experimental group based on the bin of 860 samples surveyed. Table 3.3 lists the statistics of HIC applications in the experimental group during the year of 2002. The average HIC applications in the experimental and control groups of different ages and genders are plotted in Figure 15 and listed in Table 3.4. Note that the number of using the HIC

represents the number of attending a hospital or a clinic. Apparently, deviation between the control group and experimental group is more significant as age increases. This observation demonstrates that Zen meditation practice has long term effects on health. And we might probably infer that the aging process slows down.

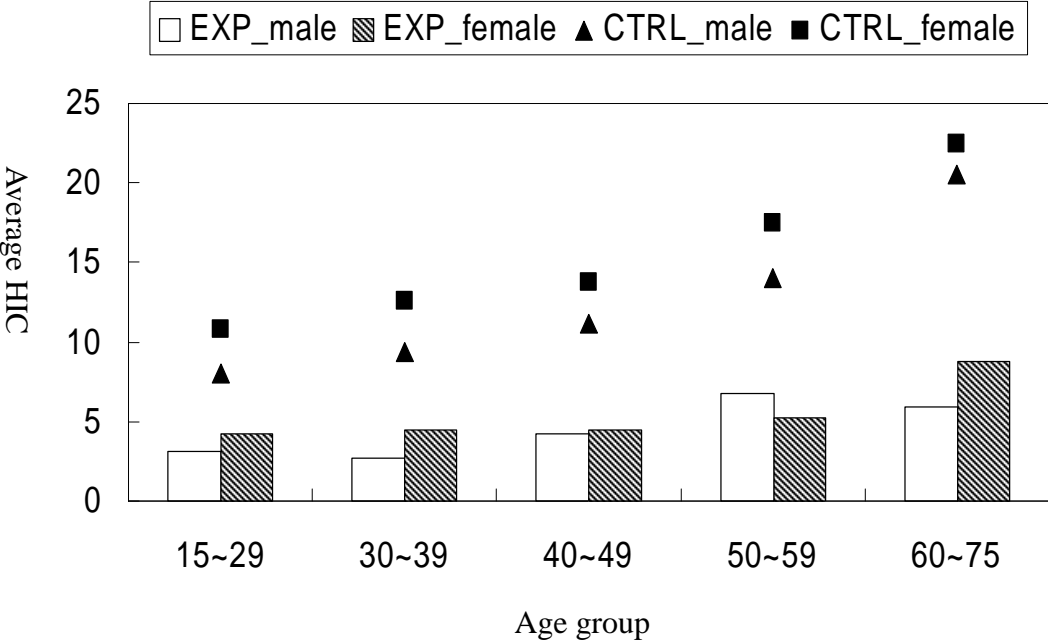


Figure 15 The average HIC applications in the experimental and control groups of different ages and genders (blank bar: EXP_male, shaded bar: EXP_female, triangle: CTRL_male, square: CTRL_female).

Table 3.3 Statistics of HIC applications in the experimental group of 860 subjects.

HIC usage (times)	0	1	2	3	4	5	6-10	11-15	>15
% of 860 subjects	21.7	11.3	13.3	8.0	6.7	4.0	26.6	3.5	5.0

Table 3.4 The average HIC applications in the experimental and control groups of different ages and genders.

Age range (years) group of subjects		15-29	30-39	40-49	50-59	60-75
		Control group	Male	8.02	9.41	11.17
Female	10.80		12.61	13.75	17.49	22.46
Experimental group	Male	3.09	2.69	4.19	6.74	5.95
	Female	4.23	4.47	4.44	5.23	8.80



Table 3.5 lists the results of investigating the effects of meditation qualities and experiences on the average HIC applications. The following comments are based on the hypothesis that the average number of HIC applications is relevant to the health condition. Part (i) manifests that increasing the weekly practicing frequency up to 7 times (that is, once per day) results in the optimal health state. According to (ii), practitioners already saw great improvement in their health when they were able to meditate for approximately one hour each time. Regarding the effect of meditation posture as shown in part (iii), significant reduction in the average HIC applications (2.8/3.5 for male/female) is observed in the practitioners capable of meditating in the full-lotus position. In fact, the meditation posture is not the only factor causing this improvement. As shown in Table 3.1, practitioners in this

particular subset (the full-lotus column) have more than seven years of meditation experiences and practice more than five times per week. It might be due to their diligence and intensive practice that enable the practitioners to sit in the full-lotus position. On the other hand, the full-lotus position is the optimal meditation posture for pushing the physiological and mental activity into the state of transcendental consciousness.

Notice that the average number of HIC applications highly correlates with the subjective evaluation of grade of contentment and stress moderation. As demonstrated in (iv) and (v) of Table 3.5, practitioners in the higher grade subsets significant reduce the use of HIC.



Figures 16 and 17 illustrate the effect of weekly practicing frequency and total practicing years on the physiological health graded by self evaluation. The value of grade ranging from 1 to 5 scores the condition varying from the worst to the best, with the mid-value (grade=3) indicating the normal, average condition. The result of grade=1 is not shown because very few subjects are within this cluster that makes the statistical analysis biased. Evidently, the number of practicing years is a core factor in promoting health. Having been practicing for more than five years, most practitioners feel themselves much healthier and younger than before

Table 3.5. Average number of HIC applications for various meditation experiences of the experimental subjects.

(i) Correlation between weekly practicing frequency and average number of HIC applications				
Weekly practicing frequency (times)	1-3	3-5	5-7	>7
Average HIC (male / female)	4.1 / 5.2	4.9 / 4.9	3.9 / 4.7	3.8 / 4.2
(ii) Correlation between meditation duration and average number of HIC applications				
Meditation duration (minutes)	≤30	30-50	50-80	>80
Average HIC	6.6	5.4	4.4	6.6
(iii) Correlation between meditation posture and average number of HIC applications				
Meditation posture	Free style	Half lotus	Full lotus	
Average HIC (male / female)	5.2 / 10.7	5.1 / 5.2	2.8 / 3.5	
(iv) Correlation between contentment grade (by self evaluation) and average number of HIC applications				
Grade of contentment	5	4	3	
Average HIC	4.3	5.1	5.5	
(v) Correlation between grade of stress moderation (by self evaluation) and average number of HIC applications				
Grade of stress moderation	5	4	3	2
Average HIC	3.7	4.6	5.4	5.8

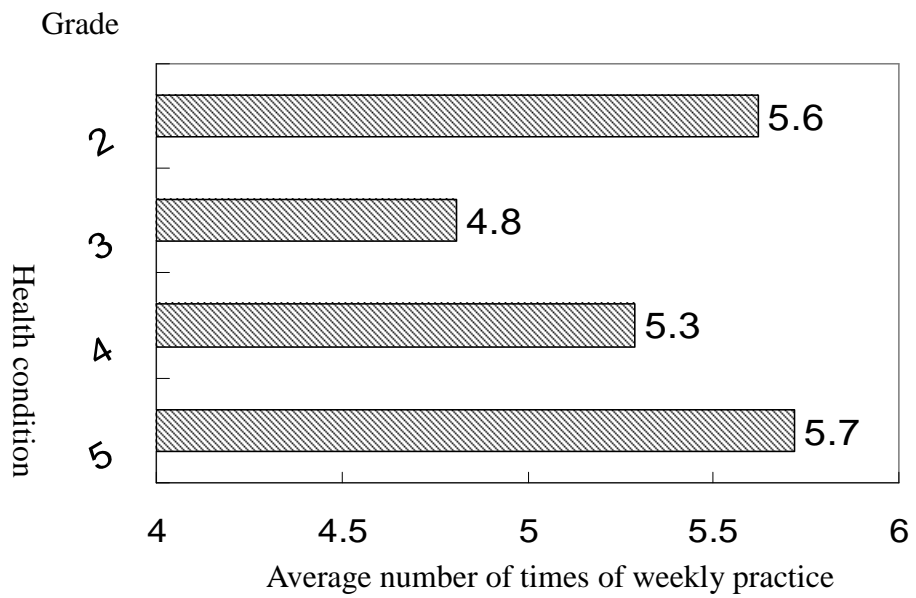


Figure 16 Effect of weekly practicing frequency on the physiological health graded by self evaluation.

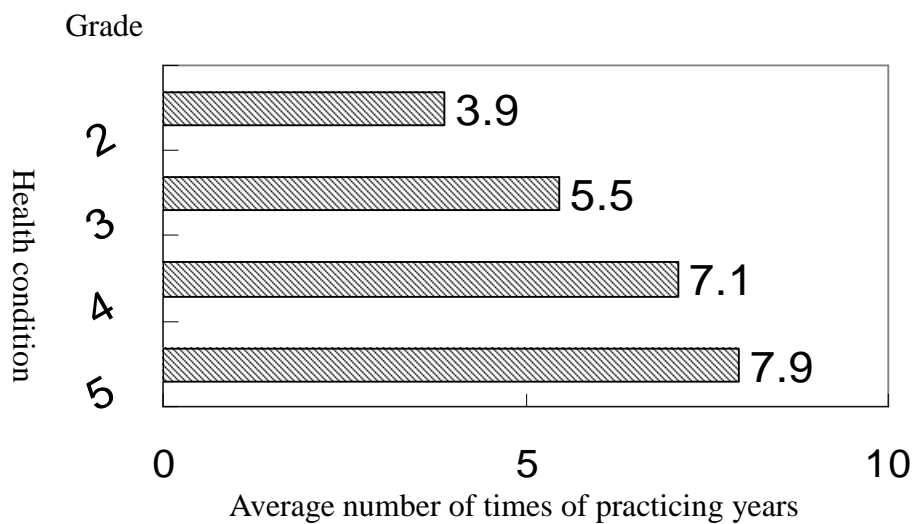


Figure 17 Effect of total practicing years on the physiological health graded by self

evaluation.

3.2 EEG alpha blocking during Zen meditation

As addressed in the Introduction, bursts of high-frequency beta (above 20Hz) were observed when the meditation practitioners entered into deep meditation. In our meditation EEG recordings, a few subjects even had significant beta activity from the beginning of meditation. This phenomenon aroused our interest in further investigating the potential mechanism. After performing a few studies on different subjects, however, we noted a significant correlation between perception of the inner light and alpha blockage. Subject A, a healthy 48-year-old man, had been practicing orthodox Zen Buddhism for more than 11 years. While meditating with eyes closed, his EEG was mainly characterized by slow-alpha (8~9 Hz) activity. A close examination showed that a tiny, high-frequency beta jiggling mingled in the alpha rhythms. When subject A signaled the event of perceiving the light, alpha blocking occurred and the EEG turned into low-amplitude beta (Figure 18). Subject B was a healthy 40-year-old female who had been practicing Zen-Buddhist meditation since 1994. Since one year after the meditation practice, she had never fallen ill. Like most Zen-Buddhist practitioners, she had an appearance and physiological status ten-years younger than her age. Her EEG in meditation switched between low-frequency ($\approx 8\text{Hz}$), high-power alpha and global beta activities, with larger amplitude in the frontal regions (F3, F4). As illustrated in Figure 19, there always occurred alpha blocking after signaling of perceiving the light.

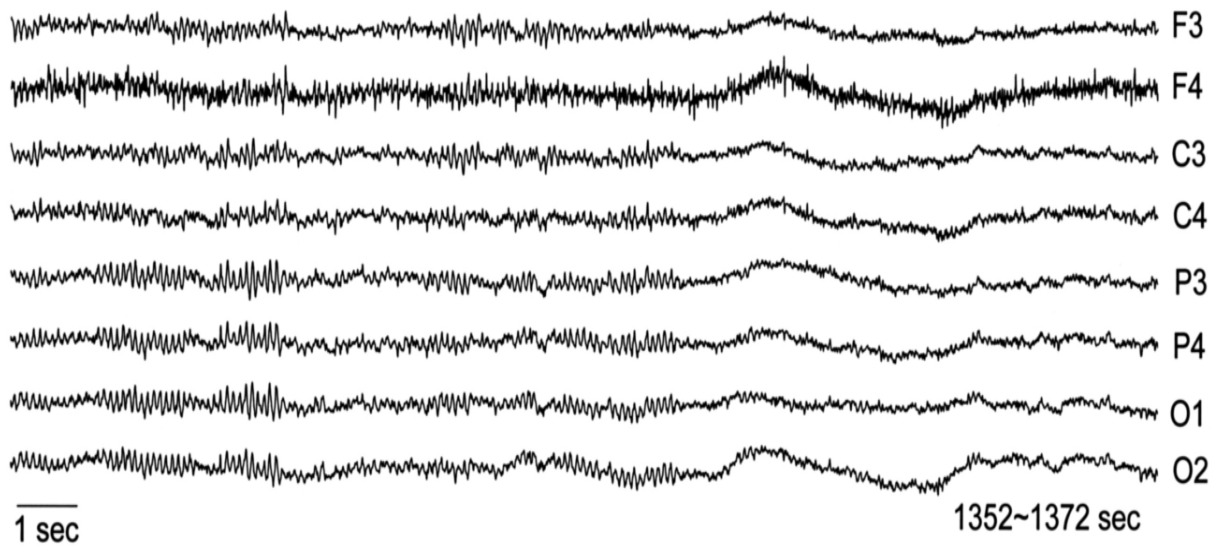


Figure 18 EEG segment of subject when perceiving the light.

Our experiment encountered one major difficulty—missing signals from the subjects. This is comprehensible since the subject when in the meditating state beyond normal consciousness often 'forgets' the experimental protocol. In these circumstances, the EEG events cannot be correlated with the meditation process via subjective expression. Overall, alpha blocking always accompanied the signaling of light perception by experimental subjects. On the other hand, we might observe alpha blocking without a preceding signal from the meditator.

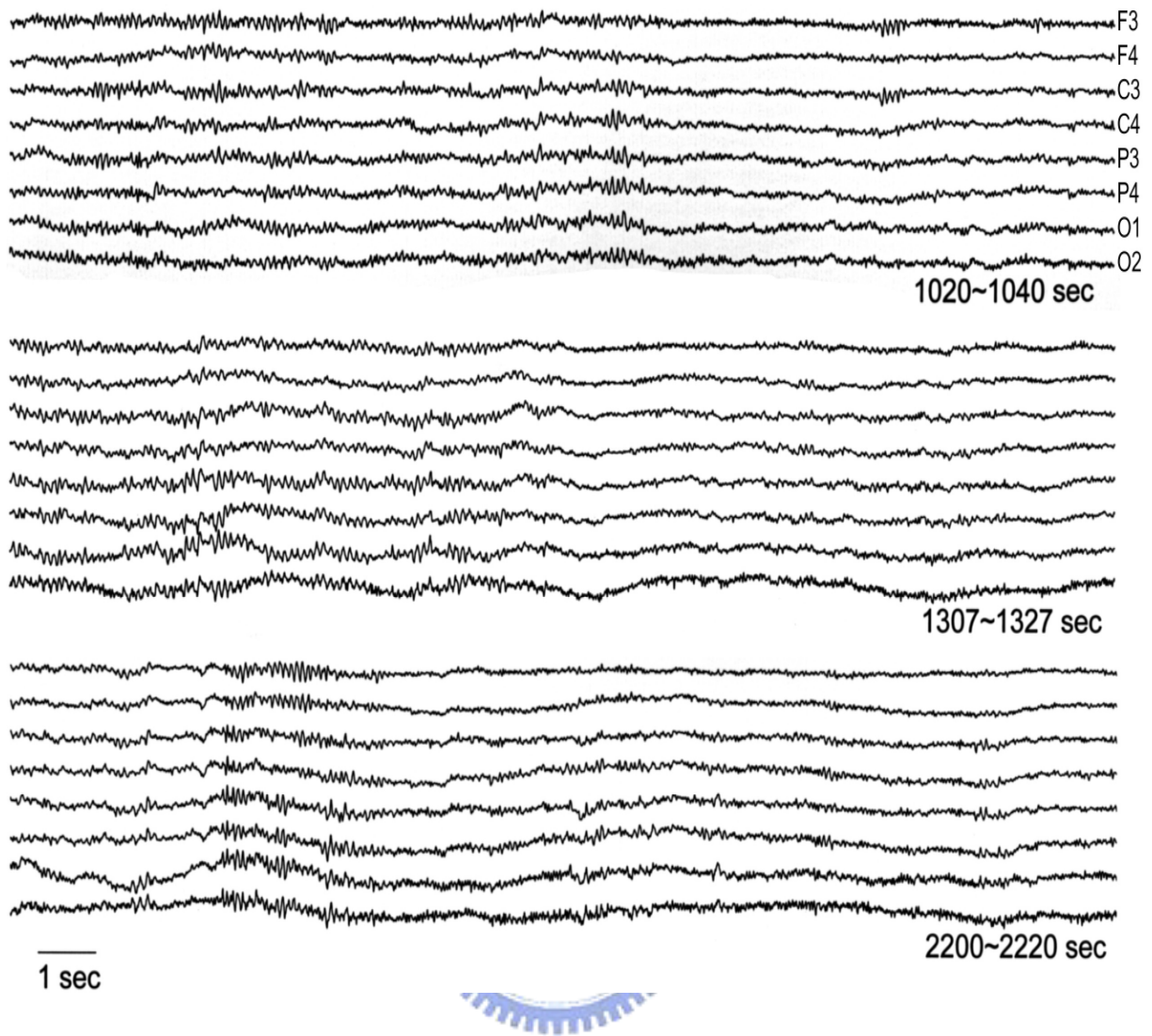


Figure 19 Three EEG segments reflecting the effect of perceiving the light

3.3 Blessing --significant alpha blocking EEG during blessings

During the blessing period, significant alpha blocking was observed in experimental subjects (C and D) and the sub-band powers of EEG during blessing are shown in Figure

20.

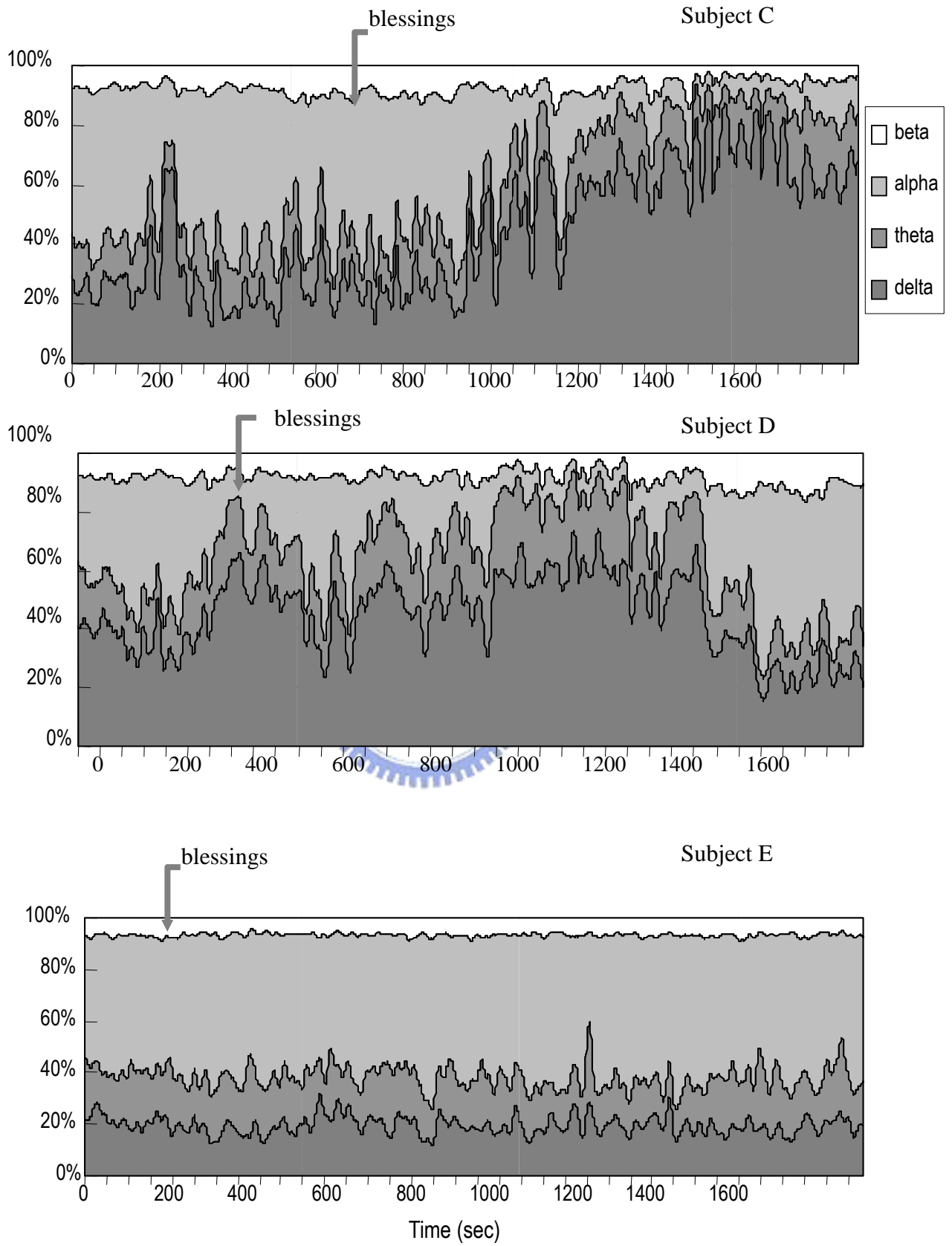


Figure 20 Running power-percentage analysis for the blessing EEG data.

We noted that the EEG of all the six experimental subjects (meditators) exhibited alpha blocking of varying degrees. This alpha blocking phenomenon was highly correlated with the fact that the subjects saw the light, according to our post-experimental interview. In the blessing period, there were the slower rhythmic activities (theta and delta). The large power of low-frequency EEG rhythms prevails over the small-amplitude beta so that the emergence of beta rhythm cannot be discriminated in the running power-percentage analysis. Apparently, there was no significant change in EEG evolution in the non-meditating control subject (E) under blessing. The EEGs of the control subjects contained a large proportion of alpha power in the entire record. In the control experiments (Figure 21), we observed that the EEGs of both subjects C and D exhibited, to some extent, alpha-blocking phenomenon which was not as evident as that observed in the blessing experiments. The result is comprehensible since, according to the result of pilot meditation EEG study, Zen-Buddhist disciples already have had their life system tuned in to the Buddhist blessings after years of meditation practice. In addition, the result of pilot meditation EEG study together with this hypothesis well explains the fact that alpha-suppression appeared in advance of the blessing ritual, as observed in subject D (Figure 20). On the other hand, the running power-percentage charts for control subject E, with and without the blessing ritual, display quite the same scenario— alpha dominates the entire EEG record.

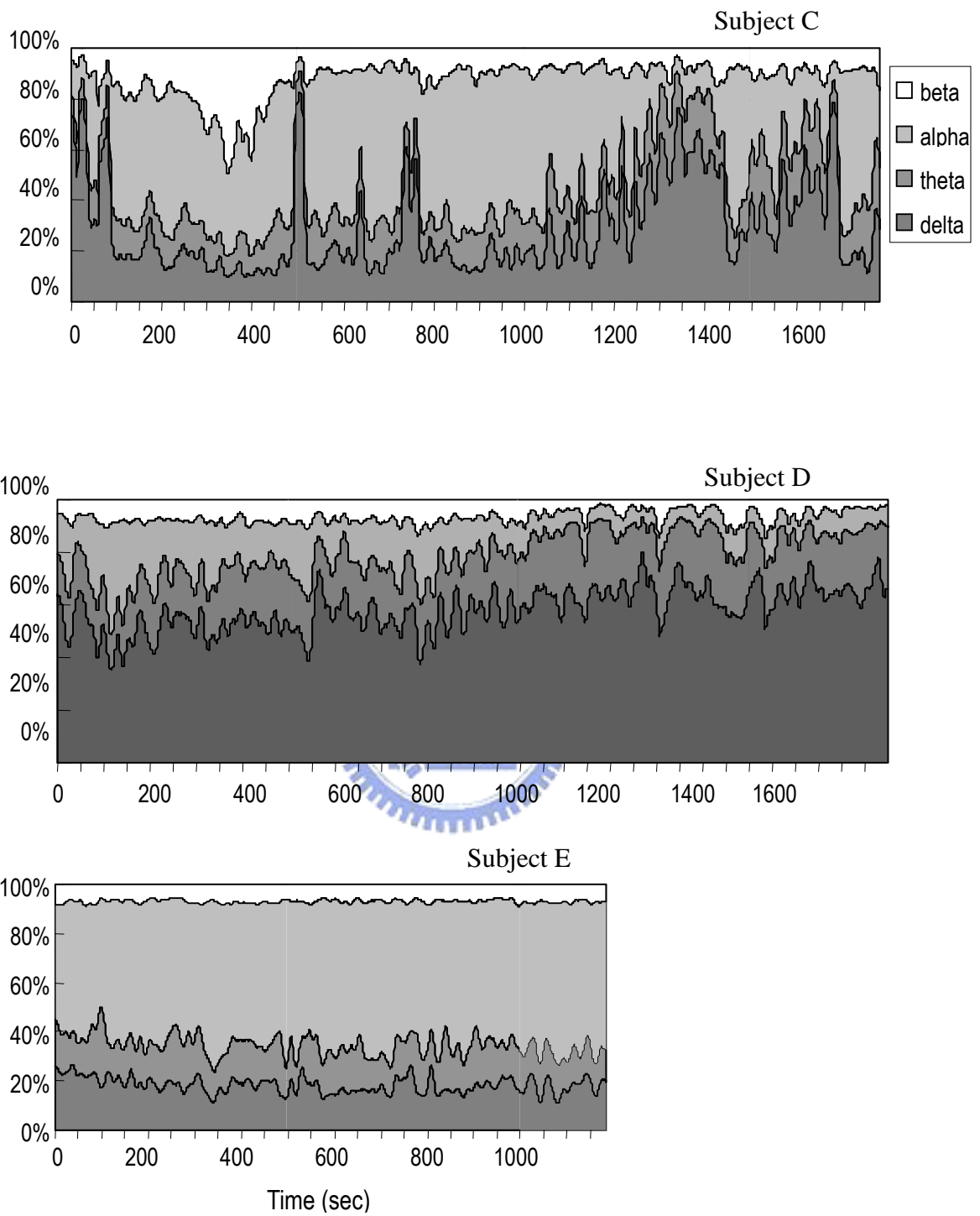



Figure 21 Running power-percentage analysis for the non-blessing EEG data.

The above experiment somehow reveals the essence of Zen-Buddhist practice— one can only sense the light of truth after years of preparation for eventually being in resonance with the inner light. During preparation, the human body itself changes its characteristics and is gradually adjusted to a state of being able to perceive this non-physical, spiritual power of blessing. In addition, we may deduce that “blessing is everywhere”, as is preached by religion, based on the results of both experiments

3.4 Meditation EEG Scenarios

3.4.1 FCM and Wavelet

3.4.1.1 Wavelet discrimination of EEG rhythm



This sub-section is intended to justify the practicability of the proposed EEG feature vectors based on wavelet decomposition. We analyze a few simulated signals, each composed of four typical EEG rhythms. These EEG segments exhibit distinctive spectral peaks, and can be easily discriminated in the plot of wavelet coefficient powers. Figure 22 illustrates the distribution of subband wavelet coefficient powers of four typical EEG rhythms. Four groups correspond to four wavelet coefficient powers, $v_7[\cdot]$, $v_6[\cdot]$, $v_5[\cdot]$, and $v_4[\cdot]$, with the length of bar indicating the range of quantifying feature $v_k[\cdot]$. In the $v_k[\cdot]$ group, the alpha, theta, delta, and flat patterns are symbolized respectively by dot, circle, asterisk, and square.

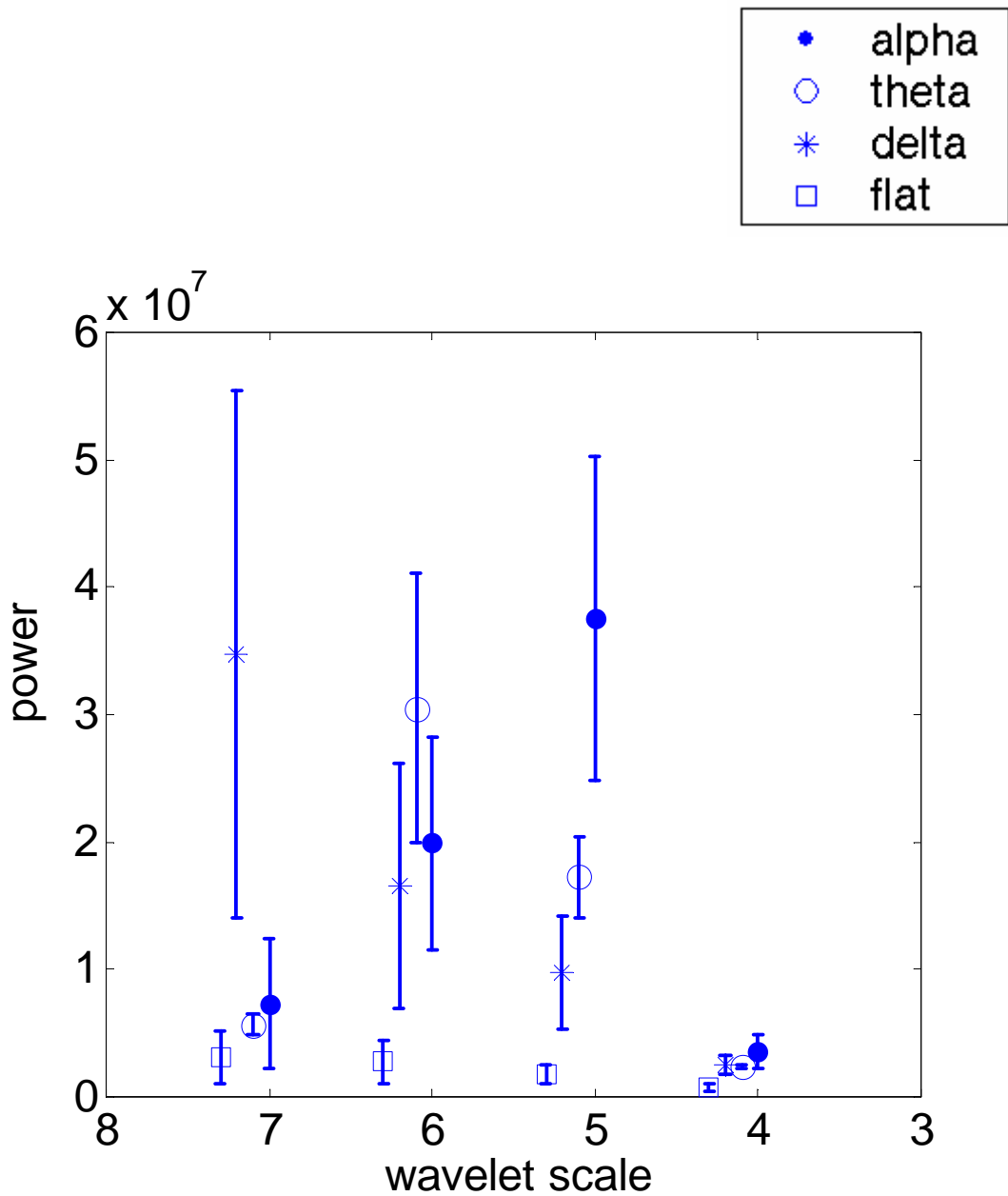


Figure 22 Distribution of subband wavelet coefficient powers (v_7 , v_6 , v_5 , and v_4).

The feature vector formulated by wavelet coefficient powers thus provides a practical medium for distinguishing various EEG rhythmic patterns. As shown in Figure 23, the 3D feature-vector space $\{v_5[\cdot], v_6[\cdot], v_7[\cdot]\}$ demonstrates that feature vectors of the same EEG

rhythmic pattern tend to gather together in the vector space. Although feature vectors of delta rhythm scatter over a larger region, further clustering-merging algorithm (FCM-merging strategies) may enhance the result of interpretation.

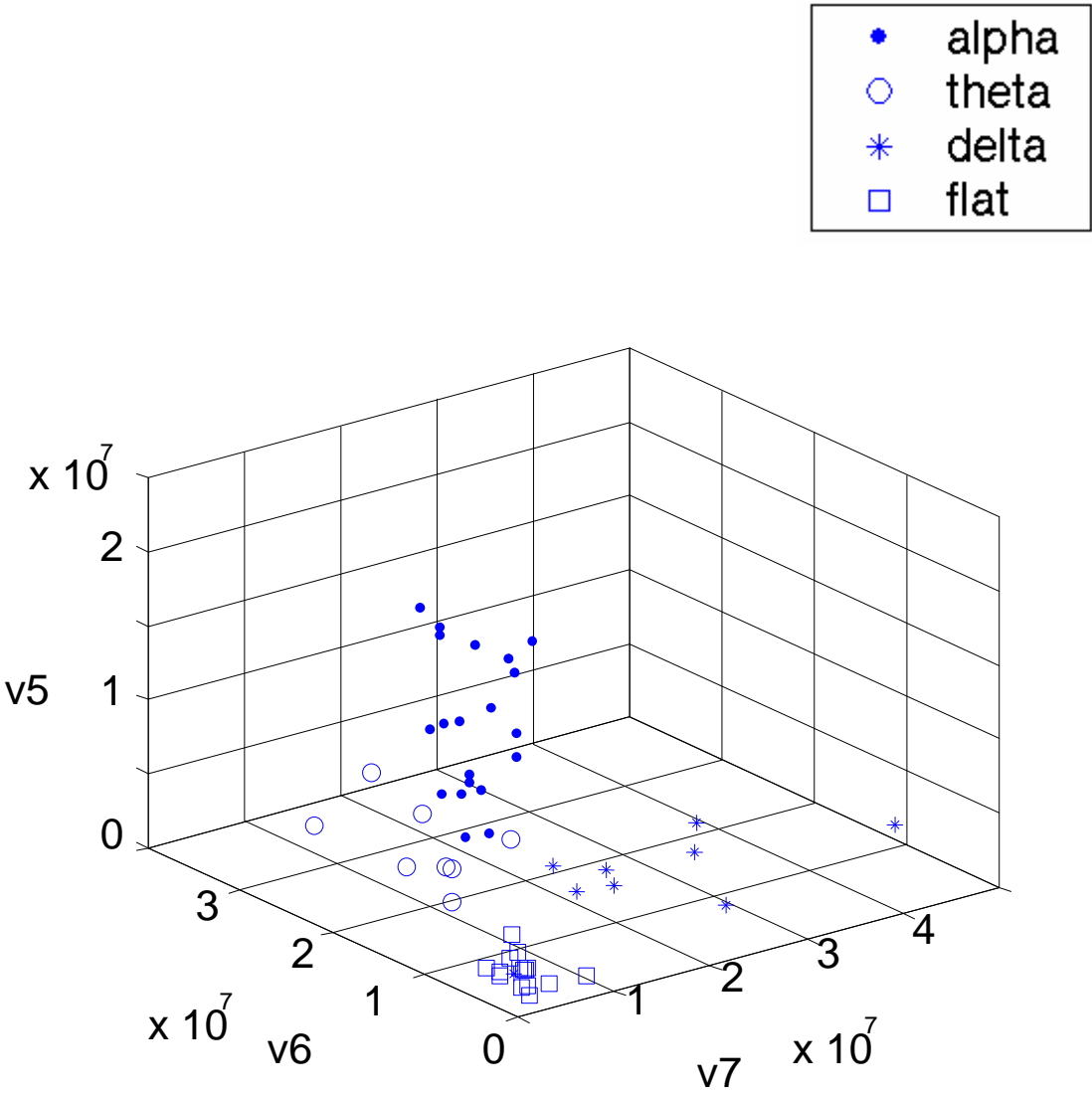


Figure 23 Three-dimensional illustration of wavelet feature vector $\{v_5[\cdot], v_6[\cdot], v_7[\cdot]\}$

3.4.1.2 Five EEG patterns in meditation

As normally characterized by its frequency, the EEG patterns are conveniently

classified into four frequency ranges: the delta (Δ , $f < 4\text{Hz}$), theta (θ , $4\text{Hz} \leq f < 8\text{Hz}$), alpha (α , $8\text{Hz} \leq f \leq 13\text{Hz}$), and beta (β , $f > 13\text{Hz}$). The meditation EEG signals, although composed of these standard rhythmic patterns, are found to orchestrate symphonies of certain tempos. After systematic study by applying the FCM-merging strategies to a number of meditation EEG data sets, results of clustering indicate that rhythmic patterns reflecting various meditation states normally involve five patterns: Δ , $\Delta+\theta$, $\theta+\text{slow } \alpha$ (denoted by $\underline{\alpha}$), high-amplitude α (denoted by α^+), and amplitude-suppressed wave. Figure 24 displays the sample patterns. Among them, the EEG pattern of particular interest is the bottom one featured by “silent and almost flat” pattern. We denote this EEG pattern with the symbol “ Φ ” in this paper.

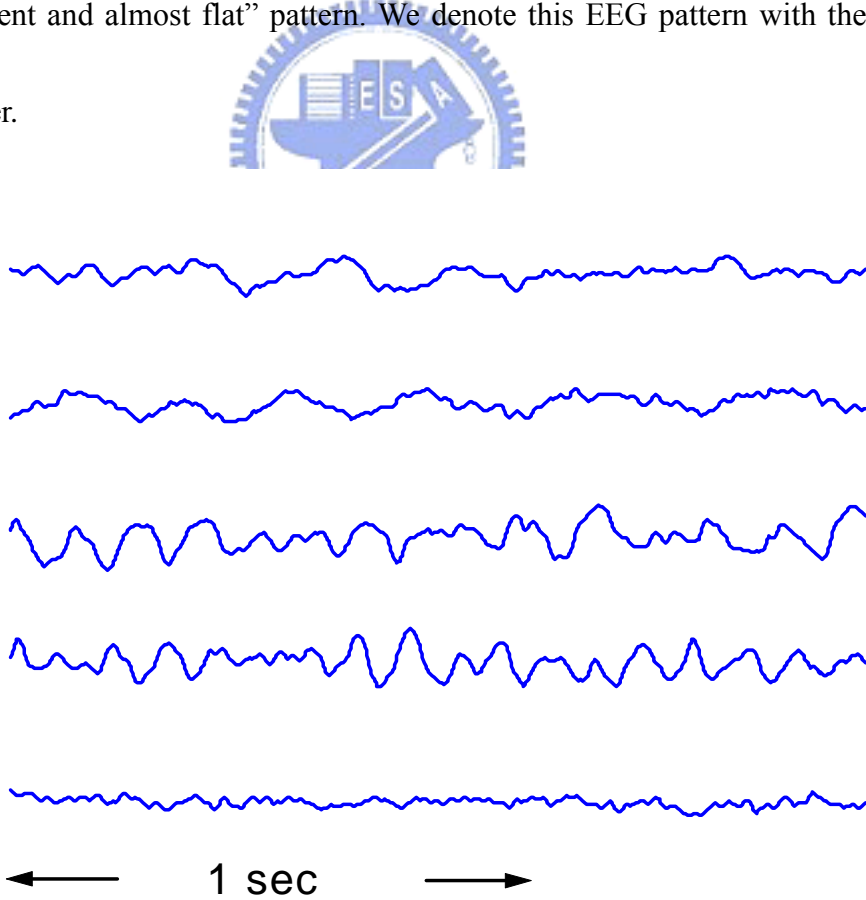


Figure 24 Five meditation-EEG patterns (from top): Δ , $\Delta+\theta$, $\theta+\underline{\alpha}$, α^+ , and Φ

Table 3.6 Subband wavelet power of five prototypes in meditation EEG.

Feature vector of different prototypes	Subband power (*10 ⁷)			
	v_7	v_6	v_5	v_4
Δ	<u>1.7044</u>	0.4623	0.3586	0.1036
$\Delta+\theta$	<u>0.9921</u>	<u>1.0543</u>	0.1564	0.0669
$\theta+\underline{\alpha}$	0.5658	<u>3.0503</u>	<u>1.7233</u>	0.2400
α^+	0.1822	1.2312	<u>2.2167</u>	0.3866
Φ	0.1115	0.1245	0.1164	0.0518

Table 3.6 lists the feature vectors for the five EEG patterns in meditation. Those dominating coefficients of each EEG patterns are underlined. In Δ patterns, v_7 significantly dominates over the others, indicating that pure Δ can be successfully classified as one cluster by the FCM-merging strategies. Similarly, α^+ patterns has largest magnitude on the v_5 feature axis, which particularly characterizes the α band (6.2~12.5 Hz). The $\Delta+\theta$ patterns is characterized by two dominating feature components, v_6 (3.1~6.2 Hz) and v_7 (1.5~3.1 Hz), due to spectral intermixture of Δ and θ . In other words, the wave shapes of both Δ and θ rhythms are not well-defined sinusoidal patterns. The θ and $\underline{\alpha}$ activities often appears simultaneously, resulting in the $\theta+\underline{\alpha}$ patterns. One unique cluster revealing particular meditation state transition is designated by the Φ patterns. Feature vectors in this cluster are

characterized by (1) extremely low power (significant suppression of EEG amplitude), (2) corresponding temporal patterns with no particular EEG rhythm, and (3) no dominating peak in the spectral distribution.

3.4.1.3 Five meditation EEG scenarios

During the past five years, we have collected the EEG and other electrophysiological signals for more than fifty meditators. Their experiences on Zen-Buddhism meditation range from a few months to sixteen years. Substantial meditation training leads them into the true Zen realm, that is, the spiritual world beyond the Alaya consciousness (the 8th consciousness). We thus are able to observe a variety of EEG changes during meditation session.



Different approaches for feature extraction may result in slight variation in interpretation of local, superficial EEG changes. Nevertheless, the quantitative illustration of whole meditation EEG record portrays a distinctive scenario for each particular meditator. To provide a long-term legible illustration, five meditation EEG patterns are displayed by different gray-scales. As illustrated in Figure 25, the gray-scales from the darkest to the brightest colors indicate, respectively, the α^+ , Δ , $\Delta+\theta$, $\theta+\alpha$, and Φ patterns. Currently, five meditation scenarios have been observed based on evolution of meditation EEG illustrated by the running gray-scale chart. We present a summing-up report below.



Figure 25 Five meditation scenarios based on evolution of meditation EEG

Meditation scenario A (Figure 25(a))— Persistent α activity dominates the entire meditation session. The Φ activities of different duration appear intermittently. According to the narration of meditators in this group (A), flights of thought continued throughout the meditation session. However, this kind of mental status would be abruptly transferred into

an entirely peaceful, serene aura. This sensation happened, mostly accompanied with feeling of light, several times in one meditation course.

Meditation scenario *B* (Figure 25(b))— Four EEG patterns, including α , Δ , θ , and Φ , appear rotationally. The meditator described the meditating sensation as follows: meditation status switched among sensations of (1) interference of mental activities, (2) alertness and tenseness, (3) subliminal status, and (4) feel of sacred, peaceful light.

Meditation scenario *C* (Figure 25(c))— EEG signals of this group are characterized by background Φ with very few α activities. Scattered Δ 's are observed. The subject is a well-experienced meditator with more than ten-year Zen practicing. In the course of meditation, she felt the energy (or light) penetrating her head several times. At the moment of energy perception, her meditation became serene and egoless. She felt the liberation from her body and mind. Nonetheless, during the entire meditation course, thoughts or drowsiness might be in and out intermittently.

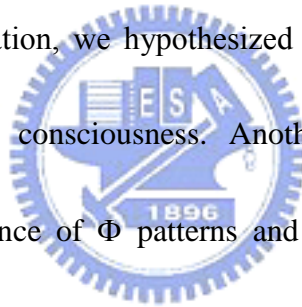
Meditation scenario *D* (Figure 25(d))— Similar to the meditation scenario *C*, however, the background Φ is sprinkled by α instead of Δ . The meditator experienced a bright (surrounded by the sacred light) and fully relaxed meditation in the test.

Meditation scenario *E* (Figure 25(e))— Their EEG's are unique. The Φ patterns dominate since the beginning of meditation, and no other activity is observed to be significant. Although the FCM-merging algorithm requires K (number of clusters) to be

larger than 2, the “cluster $i \leftarrow$ cluster j ” operation in cluster-merge C further modifies the coding vector \underline{S} according to the subband power ratios, from which a uniform activity is identified. The interpreted result highly correlates with that of the naked-eye examination.

The running gray-scale chart derived from the controlled group tells quite another story. As shown in Figure 25(f), the entire meditation scenario was dominated by the α rhythms, while $\Delta+\theta$ or θ appeared occasionally. Note that Δ and θ emerged because the subjects fell asleep. On the other hand, we observed, from the CCD video, the experimental subjects kept awake while Δ and θ emerged. This phenomenon aroused our attention.

According to the subjects’ narration, we hypothesized that Δ and θ activities are highly correlated with the subliminal consciousness. Another particular observation is the correlation between the occurrence of Φ patterns and the feeling of blessings by most experimental subjects.



3.4.2 Hurst exponent

The purpose of this section is to identify beta rhythms contained in meditation EEG data. In feature extraction and identification, an important consideration is how to avoid false-positive and true-negative classifications. A common false-positive pattern for the beta rhythm is the low-amplitude alpha rhythm, and a baseline-drifting beta wave is one of the most significant true-negative events. A low-amplitude alpha wave can often be identified

via visual inspection, but the time-domain feature parameters do not differ greatly between low-amplitude alpha waves and beta waves.

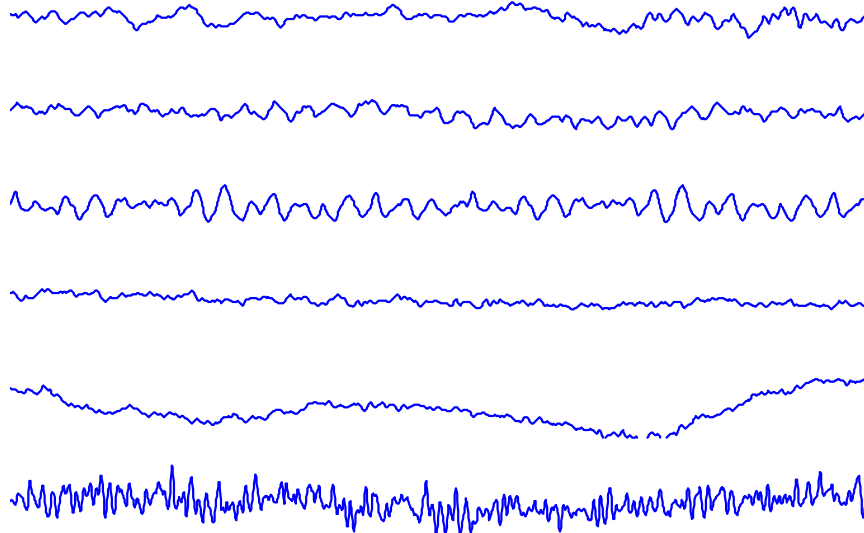


Figure 26 Time-domain EEG segments of the H&SSE pairs. From top to bottom is figure 26(a) to figure 26(f)

To demonstrate the performance of H&SSE method on the beta detection, six typical EEG rhythms of the first database are presented in Figure 26. The corresponding Fourier spectrums of the EEG rhythms are shown in Figure 27. Table 3.7 lists the resulting values of the H&SSE pair and the mean amplitude of each EEG rhythm in Figure 26.

As shown in Table 3.7, their rhythm amplitudes are similar (id #: b and d), but a low-amplitude alpha wave can be distinguished from a beta wave by its larger SSE.

The H&SSE distribution of the second database involving different EEG rhythms is

shown in Table 3.8 and Figure 28 Most beta waves have SSE values below 5, and the average SSE is 2.1. On the other hand, most alpha waves have SSE values greater than 8, and the average SSE value is 15.9. This behavior of the proposed method allows low-amplitude alpha waves to be distinguished from beta waves on the basis of their SSE values.

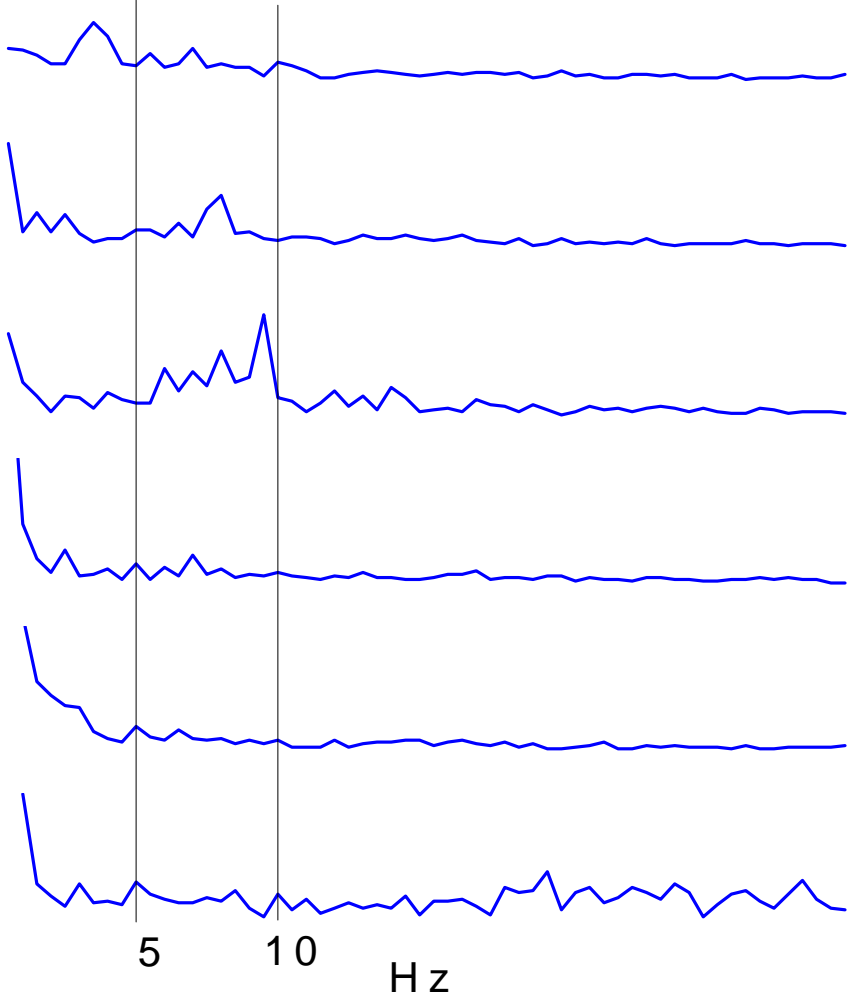


Figure 27 The corresponding Fourier spectrums of the EEG waveforms in figure 26.

Table 3.7 Corresponding H, SSE, and mean amplitude of each EEG segments

*Trace number in Figure 26. **Arbitrary units.

id number*	Test EEG rhythm	H	SSE	Amplitude**
a	Delta	0.4498	0.7349	5.915
b	Low-amplitude alpha	0.0948	8.6722	5.963
c	Normal alpha	0.0394	19.5856	9.437
d	Beta	0.0020	2.5202	5.296
e	Baseline-drift beta	0.2776	0.6356	9.690
f	High-frequency-noise-contaminated beta	-0.3959	1.1731	1.3958

Table 3.8 H and SSE distribution (mean±std for each rhythmic group) of 200 EEG epochs.

Accurate H and SSE values of each epoch are demonstrated in Figure 28

EEG rhythm	H	SSE	Number of data sets
Delta	0.3676±0.0873	2.1496±1.4539	33
Alpha	0.0733±0.0937	15.873±4.2009	57
Beta	0.0809±0.1164	2.0595±1.1451	102
Beta+noise	-0.5669±0.1216	1.2168±0.5243	8

Baseline-drifting beta may be mis-classified as delta or alpha but not beta waves for its high-amplitude values (time-domain feature) listed in Table 3.7 (id #: c and e). In frequency-domain analysis, the spectral shape in Figure 27(e), similar to that in Figure 27(a), may mislead the interpretation. This is a true-negative case of beta wave identification. The lower SSE and H values also make the beta waves distinguishable from delta and alpha waves, as indicated in Table 3.7.

Table 3.8 and Figure 28 demonstrate the distribution of H&SSE pairs for the 200 epochs in the second database. Distribution of these data exhibits special geometric

properties on the SSE-versus-H plane. The H&SSE pairs magnify the feature space of beta waves, and are located near the origin of the SSE-versus-H plane, with low positive SSE and low absolute H values. A delta wave is distinguishable from a beta wave due to its larger values of H. The H&SSE pairs of delta wave, with positive H and low SSE values, are distributed to the right of the beta region, whereas a contaminated beta wave has the H&SSE pairs occupying the left region (negative H and small SSE). However, H&SSE pairs compress the feature space of alpha and theta waves, and their larger SSE values naturally separate these waves from other EEG rhythms

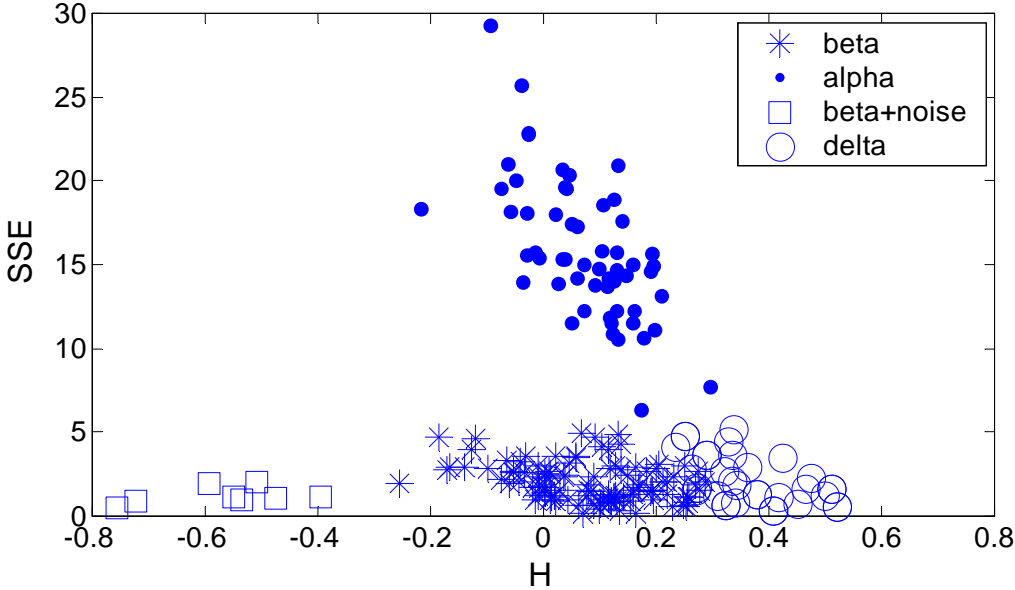


Figure 28 H&SSE pairs' distribution of long-term EEG rhythms.

The H&SSE based algorithm provides two major advantages. The first is that the H&SSE pairs depend on the particular pattern of each EEG wave, and are insensitive to the relative wave magnitudes. For example, alpha rhythms with similar waveforms shape of

different amplitude scales result in approximately steady estimate of H&SSE pairs. The algorithm is particularly robust in dealing with such variables as the recording instrument, noise interference, and biological artifacts that significantly affect the amplitude range. The other advantage of the H&SSE based algorithm is its remarkable accuracy in recognition of beta rhythm in comparison with most conventional method

The algorithm transforms the EEG rhythms into different regions on the SSE-versus-H plane and achieves a satisfactory feature-characterization performance. With the aid of sophisticated clustering algorithms, H&SSE pairs may provide a superior feature base for scoring and interpreting the long-term meditation EEG record.



3.5 Correlation between VEP and alpha-suppressed EEG

3.5.1 alpha-suppressed EEG

Figure 29 illustrates the alpha-dominated EEG (Figure 29 (a)), the typical alpha-suppressed EEG during Zen meditation (Figure 29(b)), and the corresponding power spectra (Figure 29(c)). EEG in normal relaxation with eyes closed is mostly irregular alpha, that is, amplitude envelope of alpha rhythm drifts up and down. The alpha-suppressed EEG during Zen meditation usually lasts much longer, in comparison with that during closed-eye relation. Parameters S_{max} and S_{total} (derived from equation (26) and (27)) are used to investigate the distribution of alpha-suppressed EEG duration as illustrated in Figure 30.

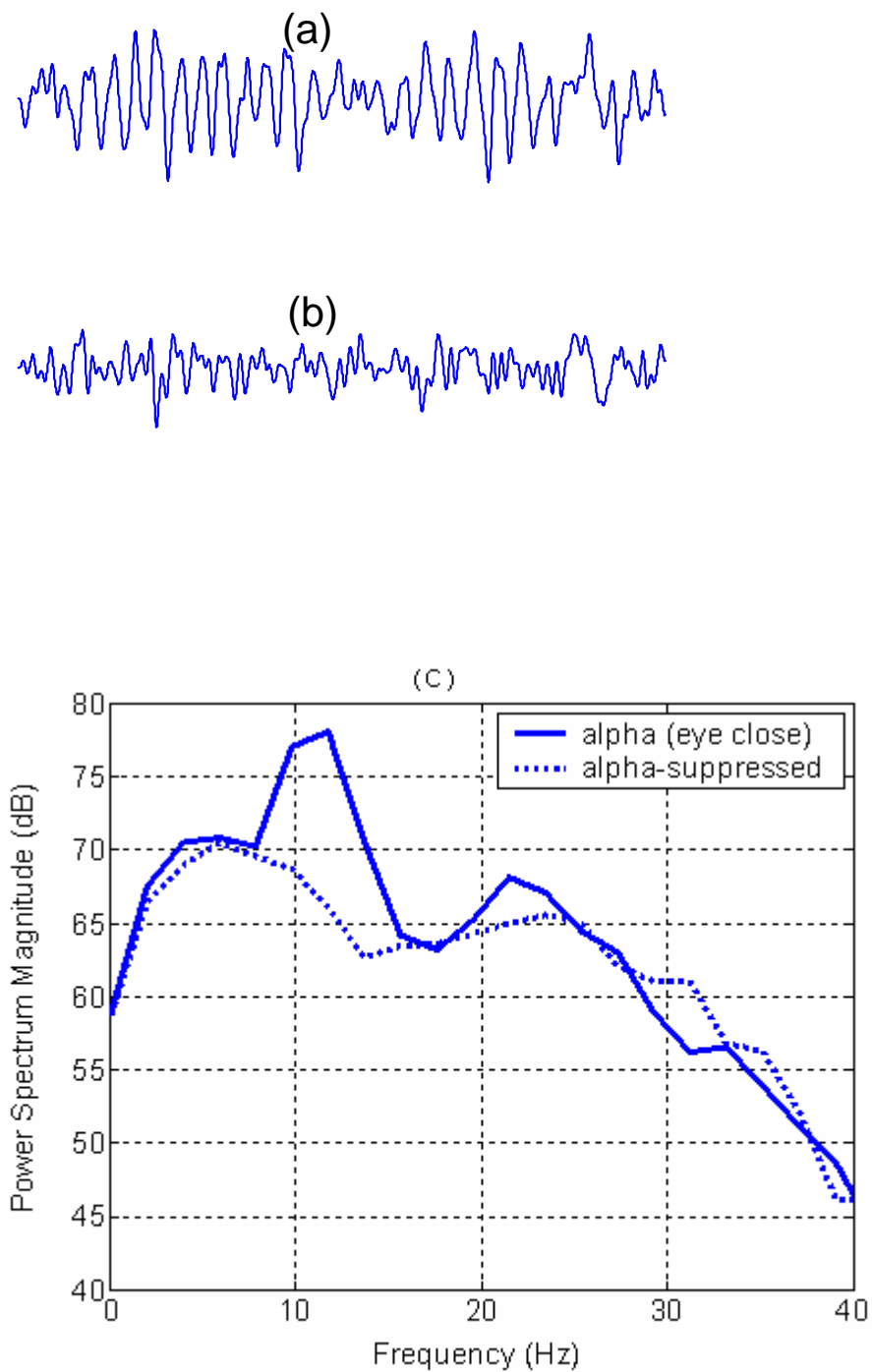


Figure 29 Typical alpha-suppressed EEG. segment and corresponding FFT spectrum

Most experimental subjects have long lasting alpha-suppressed EEG (S_{total}) that also appears in a larger proportion (S_{max}). Subjects with long-lasting alpha-suppressed EEG

often experience the inner light [48]. We may therefore infer that ranges of S_{max} and S_{total} provide a quantitative index for the deep Zen meditation state. According to Figure 30, S_{max} and S_{total} appear to be linearly dependent. They can thus be used individually to quantify the amount of alpha-suppressed EEG.

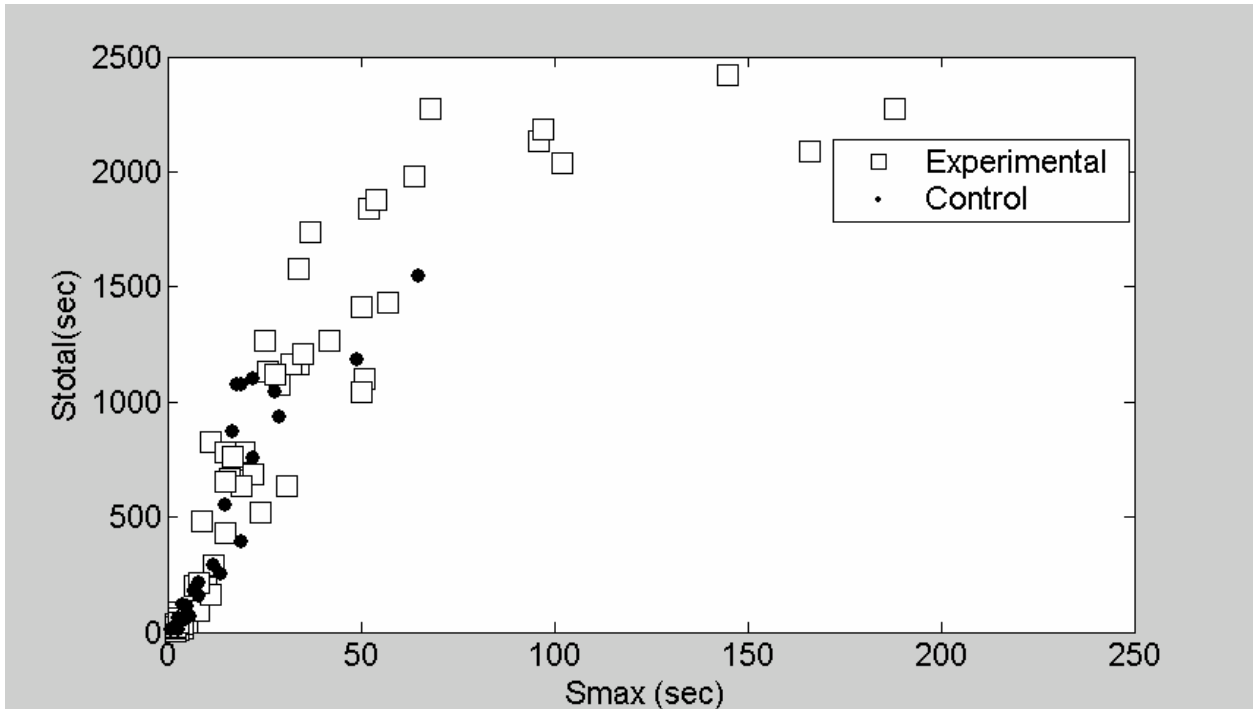


Figure 30 Illustration of sum-versus-max alpha-suppressed EEG duration

In the following discussion, we investigate the alpha-suppressed EEG by the parameter S_{max} . Figure 31 displays the average percentage of alpha-suppressed EEG for each channel (control group: vertical bars, experimental group: dotted curve). The results also reveal the fact that more alpha-suppressed EEG contents are identified for the experimental group in all the recording channels. In the experienced Zen-Buddhist practitioners, we have observed a substantial correlation between their inner light

experience and significant contents of alpha-suppressed EEG during Zen meditation. It arouses our attention to further investigate the visual stimulation response.

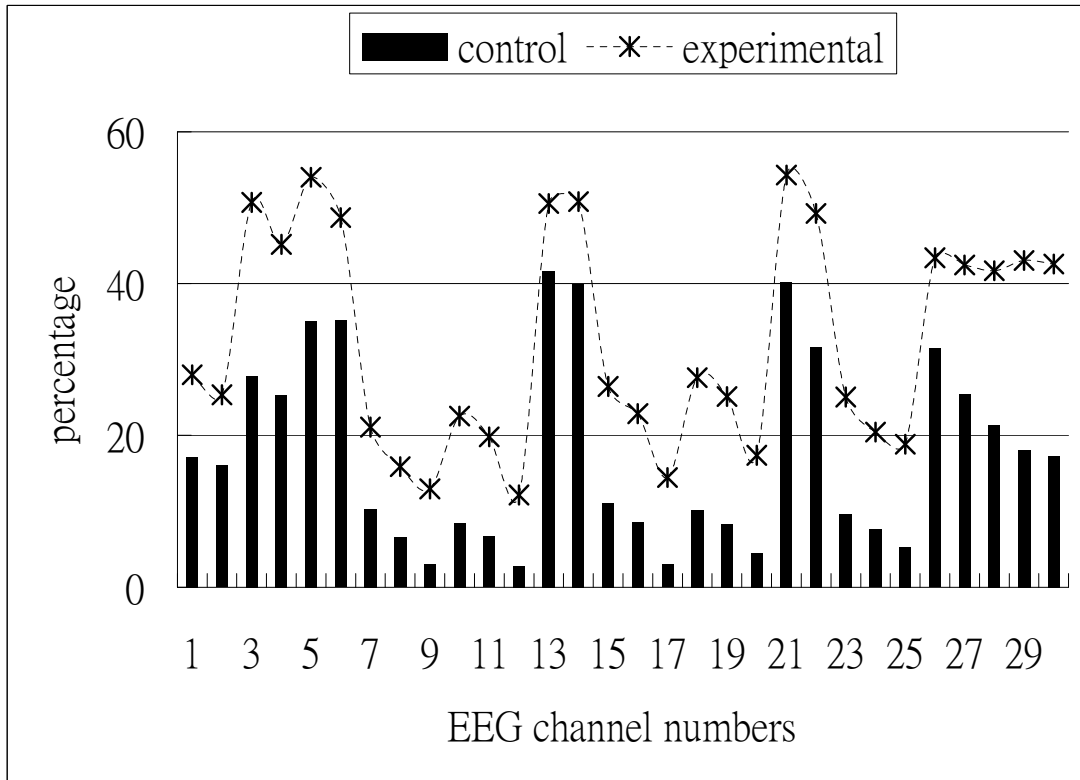


Figure 31 Average percentages of alpha-suppressed EEG

3.5.2 F-VEP

Figure 32 shows the average F-VEP patterns for the control group recorded during three recording sessions: Session I (solid curve), II (dashed curve), and III (dotted curve). The peak amplitude is measured as the difference between the absolute amplitudes of two peaks. For example, P2-N2 amplitude represents the difference between peak P2 and peak N2, denoted as P2-N2(#). The # within parentheses is the session number. Latency and amplitude are both important features charactering F-VEP in this study. However, we

observe that latencies of all the three sessions are not statistically different. We thus examine the results of F-VEP peak amplitude differences (Table 3.9). To investigate the effect of meditation/relaxation on F-VEP characteristics, Table 3.9 lists the group mean values and corresponding standard deviations (values within parentheses) of the F-VEP peak differences between sessions. We are particularly interested in the F-VEP peak amplitude differences between Session I and II (denoted as (II) – (I)) and the differences between Session III and II (denoted as (III) – (II)) of both groups.

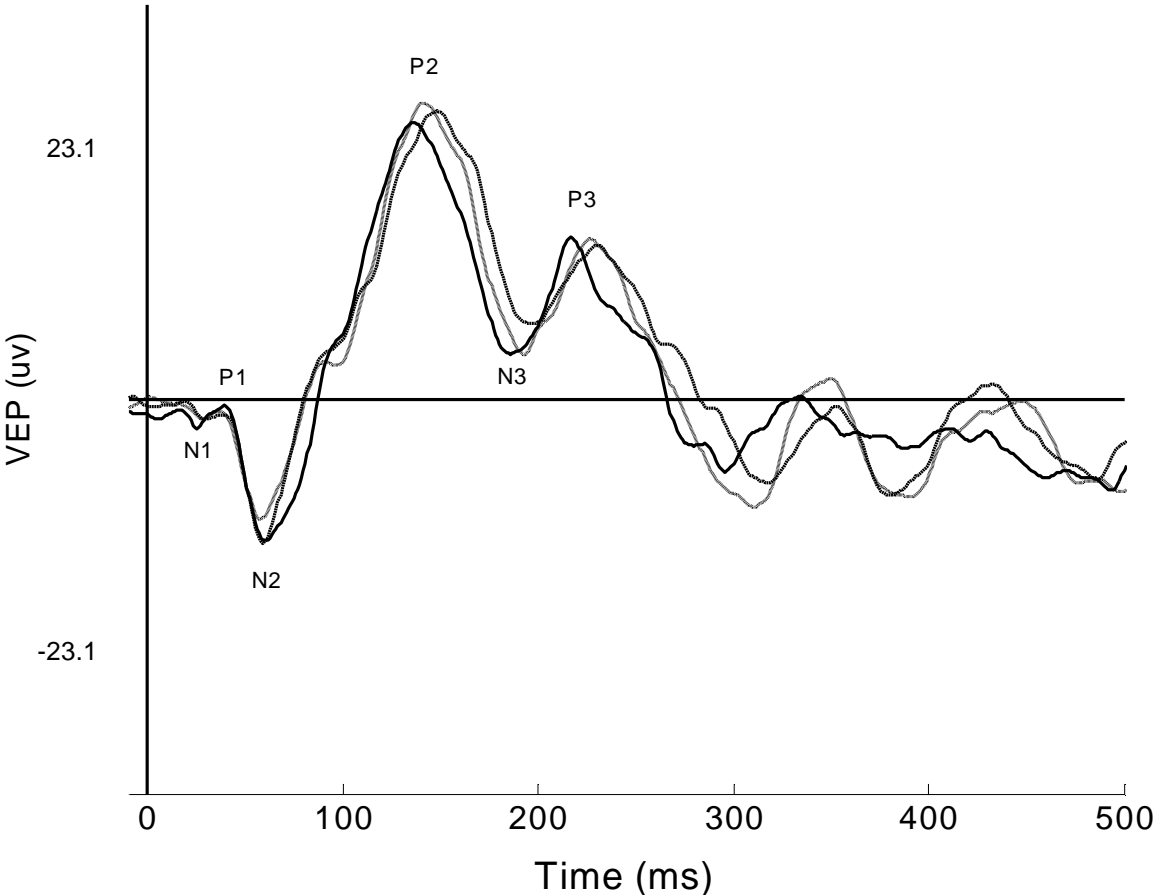


Figure 32 Average F-VEP patterns for the control group recorded during three recording sessions: Session I (solid curve), II (dashed curve), and III (dotted curve)

Table 3.9. The means (standard deviations) for the F-VEP peak amplitude difference between Session I and Session II of both groups, with P values estimated from the t-tests listed in the right column. Session I is recorded before Zen meditation (experimental group) or beginning of relaxation (control group). Session II is recorded during Zen meditation (experimental group) or middle period of relaxation (control group) .The difference (II)–(I) is from Session II value minus Session I value.

Peak	Amplitude difference	Exp (μ V)	Ctrl (μ V)	P value
		Mean(std)	Mean(std)	
P2-N2	(II) –(I)	0.364 (3.852)	2.615(6.626)	0.061
	(III) – (II)	0.675 (3.461)	0.643 (4.873)	0.972
N3-P2	(II) –(I)	-0.212 (3.274)	2.548 (5.444)	0.006**
	(III) – (II)	0.098 (2.396)	-1.071(4.884)	0.154
P3-N3	(II) –(I)	-0.493 (3.182)	1.073 (4.396)	0.061
	(III) – (II)	0.325 (2.382)	0.801 (3.113)	0.440
N4-P3	(II) –(I)	-0.936 (3.249)	0.770 (3.098)	0.025*
	(III) – (II)	0.680 (2.445)	1.322 (3.370)	0.324

Result of Table 3.9 demonstrates several features that exhibit the difference between control and experimental group. First, (II)-(I) amplitude differences of the experimental group are almost negative (P2-N2 is excluded), which are positive for the control group. The data reflecting the major differences in Session II provide substantial evidence for discriminating the meditation from the normal relaxation by the effects on F-VEP.

Second, N3-P2 and N4-P3 peak amplitudes are statistically distinct between both groups according to the small P values (0.006 and 0.025), and the absolute (II)-(I) amplitude difference of experimental group is smaller than that of the control group. Note that the F-VEP amplitude has been assumed to infer the strength of the visual nervous response; the latter F-VEP peak corresponds to the higher level of visual response that involves the cognitive and mental task. According to the above observation, we may hypothesize that Zen meditation results in decreasing cognitive involvement and lessening mental activity.

3.5.3 Feature space of EEG and F-VEP

Alpha-suppressed EEG and F-VEP data result from different visual stimulation mechanisms. In this sub-section, we investigate the distribution characteristics of the 2-dimensional feature space constructed by two parameters, S_{max} and amplitude difference (N3-P2 (II)-(I)). Figure 33 displays the quantitative features for the experimental (square) and control (dot) groups. The horizontal axis represents the S_{max} , and the vertical axis

represents the amplitude difference. There is a significant overlapped region between two groups when $S_{max} < 30$ (Figure 33). Experimental subjects with smaller S_{max} value may not experience deeper meditation state, and therefore have small S_{max} value that is similar to the control group in rest state. On the other hand, experimental subjects with larger S_{max} reflect the persistent alpha-suppression phenomenon during meditation that corroborates our previous observation. The fact is further verified by the attenuation of in-meditation N3-P2 (II) in comparison with the pre-meditation N3-P2 (I).

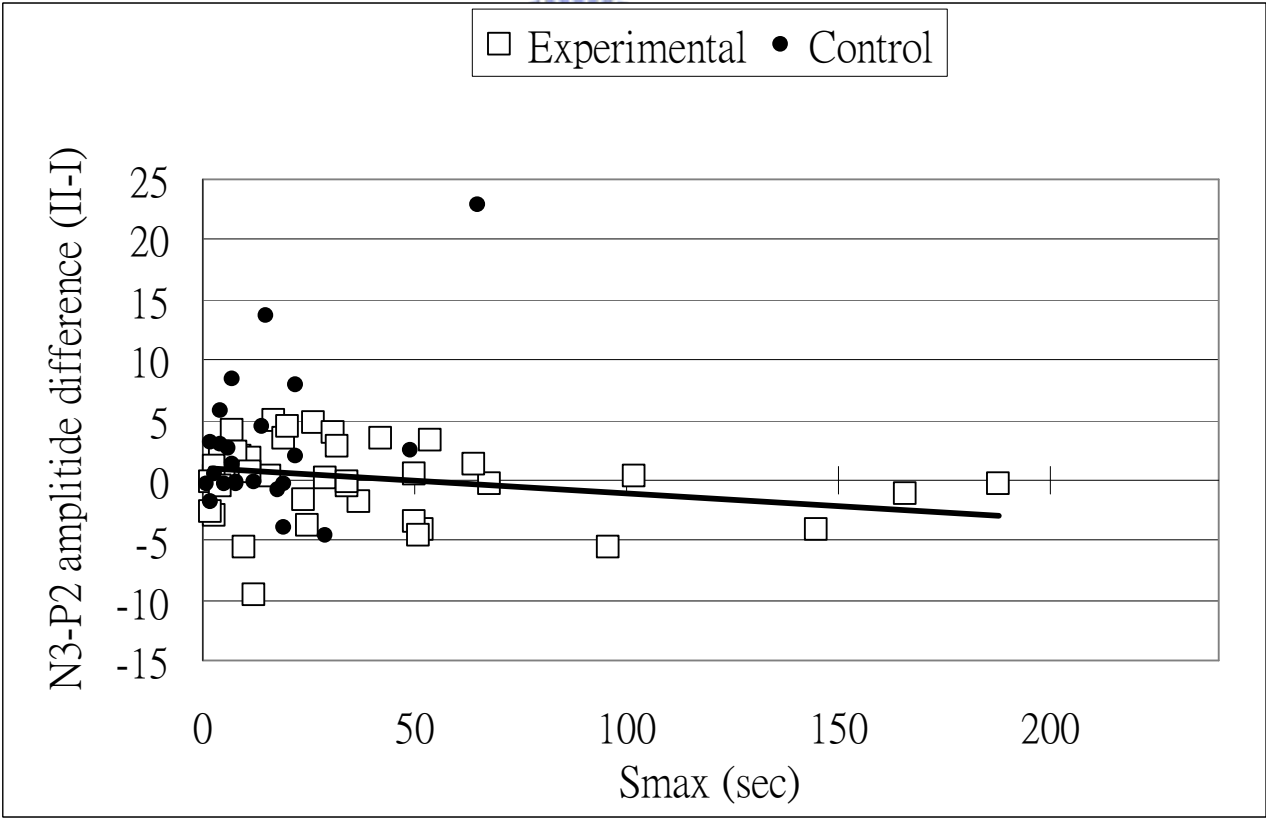


Figure 33 Maximum alpha-suppressed EEG duration versus F-VEP N3-P2 peak amplitude differences of Session II and I

Chapter 4 DISCUSSIONS AND CONCLUSION

To investigate the Zen-meditation EEG properties, the research work presented in this thesis began from the experimental setup and was devoted to the development of a number of DSP algorithms for data analysis and interpretation. The Zen-Buddhist doctrine and practitioners' experiences provide a sound basis for our proposal of a hypothesized visual neuronal mechanism under Zen meditation. First, we presented the health status of Zen practitioners. Results of field survey show that Zen meditation practitioners maintain a much better health than the non-practitioners. In the study of EEG under blessing, results indicate that spiritual resonance between the Master and disciples is an important factor to make the blessing work. In other words, brain dynamic of the disciples could attain to a state of egolessness (Alaya state) caused by blessing from the Zen Master. Control subjects (non-practitioners), without changing the physiological constitution through years of Zen resonance, however failed to respond to the blessing. Without any a priori knowledge of the Zen-meditation EEG, we developed a Fuzzy-clustering based algorithm to investigate the major EEG feature distributions.

One important finding of our study for years is the alpha-suppressed EEG pattern with low power and high frequency, which highly correlates with the experience of inner light perception. We accordingly developed a unique approach based on the Hurst-exponent evaluation to effectively extract this alpha-suppressed EEG pattern, which was unavailable

by the FCM clustering method. Moreover, F-VEP results together with the narrations of practitioners further corroborate the inner light phenomenon. Details are discussed below.

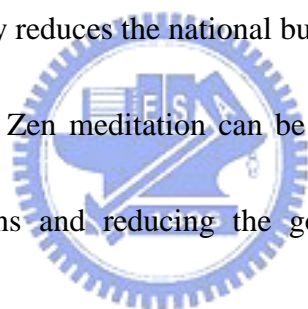
4.1 Effect of Zen meditation on health

In this report, we employed the HIC record as a basis of comparison since it is an objective, quantitative reference. In addition, this record provides a more reliable index of the health status in Taiwan than in other countries. According to our survey and statistical analysis of the results, Zen-Buddhist practitioners indeed exhibit better health in both physiological and mental conditions in comparison with the conditions before their practice. Particularly, the data of HIC applications demonstrate an impressively reduction of the average number of clinical visits by the practitioners, that helps the community save an enormous amount of expenditure on health insurance.

To sum up the surveyed data in this study, first of all, less than 20 percent of the Zen-Buddhist practitioners feel the life stress. Most practitioners (~90 percent) are well capable of moderating the occasional stresses. The mental health positively correlated with the practicing frequency and the practicing experiences (in number of years). Practitioners with more than seven-year intense practice have been capable of attaining to a totally stress-free feeling in their daily lives. The health state can be optimized by increasing the weekly practicing frequency up to 7 times. In addition, meditation duration of one hour

may lead to a great improvement in health. Significant reduction in the average HIC applications (2.8/3.5 for male/female) is observed in the practitioners capable of meditating in the full-lotus position. Moreover, the average number of HIC applications highly correlates with the subjective evaluation of grade of contentment and stress moderation. The number of practicing years is a core factor in promoting health. Having been practicing for more than five years, most practitioners feel themselves much healthier and younger than before.

Based on the results of our survey, practice of Zen meditation significantly reduces the HIC applications and accordingly reduces the national budget allocated for the Medicare. In these financially stressed times, Zen meditation can be considered an effective means of promoting health of the citizens and reducing the government expenditure on health insurance.



4.2 Principle of blessings

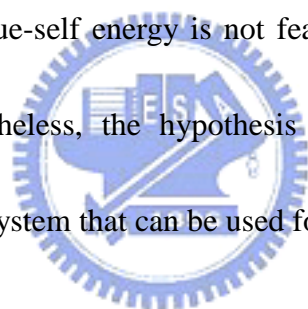
Scientific convention developed in the physical world may not allow us to explain every aspect of nature, especially those non-physical, intangible experiences developed during Zen-Buddhist practice. Nevertheless, the connection between spiritual experience and physical phenomenon can be explored via the medium of the human life system. In this blessing experiment, we report a reasonable hypothesis that correlates alpha-blocking

phenomena with perception of the inner light of true self. The phenomenon of alpha blocking in human subjects, having long been of interest, may be induced by mental arithmetic, tension or otherwise in addition to the well-known eye-opening test [99]. This is the first report of alpha blocking during meditation rather than the mental and visuomotor tasks studied by most researchers. At the onset of the light-perceiving experience during meditation, the alpha-dominated background EEG turns into a small-amplitude beta rhythm, or becomes flat with its amplitude significantly suppressed.

Perceiving the inner light, as stated by the practitioners, makes them feel they are being blessed by the inner energy of true self. This is one of the experiences discovered by orthodox Zen-Buddhist practitioners on the way towards unification of the physical, mental, and spiritual (true-self) entities. This kind of experience enables them to remain in a serene, unified, and ecstatic state of mind. It works like a sudden illumination that releases their mind from the inextricable maze. As a result, they gain great health after years of practicing. The idea is that we may promote our health via disclosure of this inner energy. This report provides a new insight into the debate that meditation benefits physiological, psychological, and mental health.

In the blessing experiment, alpha blockage appears to have poor temporal correlation with the blessing ritual. Mechanisms of blessing are still undefined from the scientific viewpoint. However, we may hypothesize, based on qualitative descriptions [5]-[6], that

true blessing is actually performed on the spiritual being. Accordingly, recording of electrophysiological signals involves a transducing process from the spiritual to the physical domain. Poor temporal correlation is thus likely. Nevertheless, the running power-percentage charts show significant effects of blessing for meditators, whereas the results for non-meditators indicate alpha-dominated EEGs no matter whether blessing was applied. Note that the Chakras (Figure 3) involved in the perception of inner light are located near the visual perceptive pathway. May we hypothesize that the alpha blocking relates to visual attention to the inner light? The inference is still primitive since direct validation or detection of the true-self energy is not feasible in the present scientific and technical circumstances. Nonetheless, the hypothesis is substantially sound based on recordings from the human life system that can be used for corroborating this energy.



4.3 Meditation EEG patterns and meditation scenarios

As the transition of consciousness states in meditation is still a myth, this paper reports a novel idea of understanding various meditation scenarios via EEG interpretation. Instead of the θ trains and α^+ rhythms observed in the TM deep meditation [42], our finding shows that substantial EEG power suppression (Φ prototype), sometimes accompanied with β rhythms, represents the most significant feature characterizing the sacred, unified, egoless, and blessed meditation stage in the orthodox Zen-Buddhism group. Experimental subjects'

narration further corroborates, from the macroscopic viewpoint, the results of EEG interpretation obtained by the FCM-merging strategies. Without pre-specified prototypical EEG features, the FCM clustering method automatically identifies the significant features to be used as the meditation EEG interpreting protocol. Sophisticated merging strategies, developed according to the experiences of naked-eye EEG interpretation, further compensate for the intrinsic deficiency of background knowledge and bring the interpretations by the human and the computer closer together.

4.4 Inner light nature of Zen meditation practice

In comparison with the alpha suppression for normal subjects when opening eyes [50], the Zen-Buddhist practitioners also exhibit the same alpha-suppressed EEGs during Zen meditation, yet, with eyes closed. One question arises: what would be the genuine mechanism of alpha suppression during meditation? Is it possibly caused by the mental activities? According to our study on each experimental subject, alpha-suppressed EEGs that were caused by mental activity exhibit higher alpha contents than those during meditation.

The large inter-subjects variation of F-VEP results in the difficulty and insignificance of analyzing raw data [81]. Since the main aim of this study was to investigate the effect of meditation, we thus focused on the difference of amplitude. In the experimental group,

N3-P2 peak amplitude varies little from the pre-meditation (I) to the in-meditation (II) session, and finally to the post-meditation (III) session. It reflects a well stabilized visual neuronal system that is affected little by the outside environmental stimuli.

According to the Zen-Buddhist practice [5]-[6], the experienced practitioners being in resonance with their true wisdom are capable of attaining the highest level of qi (the light aureola) that was described as the inner-light experience [48]. It was reported that Christian or Catholic when praying deeply with God also had the experiences of light perception. The data shown in this paper provide a connection between the subjective experiences of inner light and the physiological phenomena. To the best of our knowledge, it is the first attempt to report this finding academically.



REFERENCES

- [1] Fields JZ, Walton KG, Schneider RH, Nidich S, Pomerantz R, Suchdev P, Castillo-Richmond A, Payne K, Clark ET and Rainforth M. Effect of a multimodality natural medicine program on carotid atherosclerosis in older subjects: a pilot trial of Maharishi Vedic Medicine. *American Journal of Cardiology* 2002; 89(8):952-958.
- [2] Ghassemi J. Finding the evidence in CAM: a student's perspective. *Evidence Based Complementary and Alternative Medicine* 2005 Sep;2(3):395-397.
- [3] Majumdar M, Grossman P, Dietz-Waschkowski B, Kersig S and Walach H. Does mindfulness meditation contribute to health? Outcome evaluation of a German sample. *Journal of Alternative and Complementary Medicine* 2002; 8(6):719-730.
- [4] <http://nccam.nih.gov/health/whatiscam/#sup1#sup1>
- [5] Wu Jue Miao Tian. *Introduction to Zen Meditation* (Chinese). Zen Cosmos Publish Ltd., Taiwan, 2004,
- [6] Wu Jue Miao Tian. *Zen Wisdom* (Chinese). Taiwan Zen Buddhist Association, Taiwan: Taipei, 2000.
- [7] Lee MS, Rim YH and Kang CW. Effects of external qi-therapy on emotions, electroencephalograms, and plasma cortisol. *International Journal of Neuroscience* 2004 Nov; 114(11): 1493-1502.

- [8] Lu Z. *Scientific qigong exploration – The wonders and mysteries of qi*. Malvern, PA: Amber Leaf Press, 1997.
- [9] Silva LM and Cignolini A. A medical qigong methodology for early intervention in autism spectrum disorder: a case series. *American Journal of Chinese Medicine* 2005; 33(2):315-327.
- [10] Wallace RK. Physiological effects of transcendental meditation. *Science* 1970; 167:1751–1754.
- [11] Bennett JE and Trinder J. Hemispheric laterality and cognitive style associated with transcendental meditation. *Psychophysiology* 1997; 14(3): 293-296.
- [12] Hebert R and Lehmann D. Theta bursts: An EEG pattern in normal subjects practicing the transcendental meditation technique. *Electroencephalography and Clinical Neurophysiology* 1997;42(3): 397-405.
- [13] Becker DE and Shapiro D. Physiological responses to clicks during Zen, Yoga, and TM meditation. *Psychophysiology* 1981; 18(6): 694-699.
- [14] Stigsby B, Rodenberg JC and Moth HB. Electroencephalographic findings during mantra meditation (transcendental meditation). A controlled, quantitative study of experienced meditators. *Electroencephalography and Clinical Neurophysiology* 1981; 51(4): 434-442.
- [15] Heide FJ. Psychophysiological responsiveness to auditory stimulation during transcendental meditation. *Psychophysiology* 1986; 23(1): 71-75.

- [16] Jevning R, Wallace RK and Beidebach M. The physiology of meditation: a review. A wakeful hypometabolic integrated response. *Neuroscience and Biobehavioral Reviews* 1992; 16(3): 415-424.
- [17] Istratov EN, Liubimov NN and Orlova TV. Dynamic features of the modified state of consciousness during transcendental meditation. *Bulletin of Experimental Biology and Medicine* 1996; 121(2): 128-130.
- [18] Travis F, Olson T, Egenes T and Gupta, HK. Physiological patterns during practice of the Transcendental Meditation technique compared with patterns while reading Sanskrit and a modern language *International Journal of Neuroscience* 2001;109 (1-2):71-80.
- [19] Travis F. Autonomic and EEG patterns distinguish transcending from other experiences during Transcendental Meditation practice. *International Journal of Psychophysiology* 2001; 42 (1): 1-9.
- [20] Travis F, Arenander A and DuBois D. Psychological and physiological characteristics of a proposed object-referral/self-referral continuum of self-awareness. *Consciousness and Cognition : an International Journal* 2004 Jun;13(2):401-420.
- [21] Travis F, Tecce J, Arenander A and Wallace RK. Patterns of EEG coherence, power, and contingent negative variation characterize the integration of transcendental and waking states. *Biological Psychology* 2002 Nov;61(3): 293-319.
- [22] Travis F and Arenander A. EEG asymmetry and mindfulness meditation.

Psychosomatic Medicine 2004 Jan-Feb; 66(1): 147-148.

[23] Anand BK. Yoga and medical sciences. *Indian J Physiol Pharmacol* 1991Apr;35(2): 84-87.

[24] Elson BD, Hauri P and Cunis D. Physiological changes in yoga meditation. *Psychophysiology* 1977 Jan;14(1):52-57.

[25] DiBenedetto M, Innes KE, Taylor AG, Rodeheaver PF, Boxer JA, Wright HJ and Kerrigan DC. Effect of a gentle Iyengar yoga program on gait in the elderly: an exploratory study. *Archives of Physical Medicine and Rehabilitation* 2005 Sep;86(9):1830-1837.

[26] Brown RP and Gerbarg PL. Sudarshan Kriya Yogic Breathing in the Treatment of Stress, Anxiety, and Depression: Part II-Clinical Applications and Guidelines. *Journal of Alternative and Complementary Medicine* 2005 Aug;11(4):711-717.

[27] Litscher G, Wenzel G, Niederwieser G and Schwarz G. Effects of QiGong on brain function. *Neurological Research* 2001; 23(5):501-505.

[28] Rapgay L, Rinpoche VL and Jessum R. Exploring the nature and functions of the mind: a Tibetan Buddhist meditative perspective. *Progress in Brain Research* 2000; 122:507-515.

[29] Takahashi T, Murata T, Hamada T, Omori M, Kosaka H, Kikuchi M, Yoshida H and Wada Y. Changes in EEG and autonomic nervous activity during meditation and their association with personality traits. *International Journal of Psychophysiology* 2005

Feb;55(2):199-207.

[30] Murata T, Takahashi T, Hamada T, Omori M, Kosaka H, Yoshida H and Wada Y.

Individual trait anxiety levels characterizing the properties of zen meditation.

Neuropsychobiology 2004; 50(2): 189-194.

[31] Woolfolk RL. Psychophysiological correlates of meditation. *Archives of General*

Psychiatry 1975 Oct;32(10):1326-1333.

[32] Kubota Y, Sato W, Toichi M, Murai T, Okada T, Hayashi A and Sengoku A. Frontal

midline theta rhythm is correlated with cardiac autonomic activities during the

performance of an attention demanding meditation procedure. *Cognitive Brain*

Research 2001; 11(2): 281-287.

[33] Staples JK and Gordon JS. Effectiveness of a mind-body skills training program for

healthcare professionals. *Alternative Therapies in Health and Medicine* 2005

Jul-Aug;11(4):36-41.

[34] Barnes VA, Bauza LB and Treiber FA. Impact of stress reduction on negative school

behavior in adolescents. *Health and Quality of Life Outcomes* 2003; 1: 10.

[35] Kjaer TW, Bertelsen C, Piccini P, Brooks D, Alving J and Lou HC. Increased

dopamine tone during meditation-induced change of consciousness. *Cognitive Brain*

Research 2002 Apr; 13(2): 255-259.

[36] King MS, Carr T and D'Cruz C. Transcendental meditation, hypertension and heart

disease. *Australian Family Physician* 2002 Feb; 31(2):164-168.

- [37] Davidson RJ, Kabat-Zinn J, Schumacher J, Rosenkranz M, Muller D, Santorelli SF, Urbanowski F, Harrington A, Bonus K and Sheridan JF. Alterations in brain and immune function produced by mindfulness meditation. *Psychosomatic Medicine* 2003 Jul-Aug; 65(4): 564-570.
- [38] Yu T, Tsai HL and Hwang ML. Suppressing tumor progression of in vitro prostate cancer cells by emitted psychosomatic power through Zen meditation. *American Journal of Chinese Medicine* 2003; 31(3):499-507.
- [39] Jevning R, Wallace RK and Beidebach M. The physiology of meditation: A review : A wakeful hypometabolic integrated response. *Neuroscience and Biobehavioral Reviews* 1992 Fall; 16(3): 415-424.
- [40] Peng CK, Henry IC, Mietus JE, Hausdorff JM, Khalsa G, Benson H and Goldberger AL. Heart rate dynamics during three forms of meditation. *International Journal of Cardiology* 2004 May; 95(1):19-27.
- [41] Cysarz D and Bussing A. Cardiorespiratory synchronization during Zen meditation. *European Journal of Applied Physiology* 2005 Jun 7.
- [42] Banquet JP. Spectral analysis of the EEG in meditation. *Electroencephalography and Clinical Neurophysiology* 1973 Aug; 35(2):143-151.
- [43] Aftanas LI and Golocheikine SA. Human anterior and frontal midline theta and lower alpha reflect emotionally positive state and internalized attention: high-resolution EEG investigation of meditation. *Neuroscience Letters* 2001 Sep; 310(1): 57-60.

- [44] Aftanas LI and Golocheikine SA. Non-linear dynamic complexity of the human EEG during meditation. *Neuroscience Letters* 2002 Sep; 330(2):143-146.
- [45] Aftanas LI and Golosheykin SA. Impact of regular meditation practice on EEG activity at rest and during evoked negative emotions. *International Journal of Neuroscience* 2005 Jun; 115(6): 893-909.
- [46] Kim YY, Choi JM, Kim SJ, Park SK, Lee SH and Lee HK. Changes in EEG of children during brain respiration-training. *American Journal of Chinese Medicine* 2002; 30 (2-3): 405-417.
- [47] Lutz A, Greischar LL, Rawlings NB, Ricard M and Davidson RJ. Long-term meditators self-induce high-amplitude gamma synchrony during mental practice. *Proceedings of the National Academy of Sciences of the United States of America* 2004 Nov; 101(46): 16369-16373.
- [48] Lo PC, Huang ML and Chang KM. EEG Alpha Blocking Correlated with Perception of Inner Light During Zen Meditation. *American Journal of Chinese Medicine* 2003; 31(4): 629-642.
- [49] West MA. Meditation and the EEG. *Psychological Medicine* 1980 May; 10(2):369-375.
- [50] Haas LF. Hans Berger (1873-1941), Richard Caton (1842-1926), and electroencephalography. *Journal of Neurology Neurosurgery and Psychiatry* 2003 Jan;74(1):9

- [51] Cooper R, Osselson JW and Shaw JC. *EEG Technology*. 3rd ed., Butterworth Inc., Woburn, MA, 1980.
- [52] Smith JR. *Automated analysis of sleep EEG data*, *Handbook of Electroencephalography and Clinical Neurophysiology*, 2 (chapter 4), Lopes Da Silva FH et al. ed., Elsevier Science Publishers, 1986.
- [53] Niedermeyer E and Lopes Da Silva FH. *Electroencephalography: Basic Principles, Clinical Applications, and Related Fields*. 4th ed., Williams & Wilkins, USA, 1999.
- [54] Oohashi T, Kawai N, Honda M, Nakamura S, Morimoto M, Nishina E and Maekawa T. Electroencephalographic measurement of possession trance in the field. *Clinical Neurophysiology* 2002 Mar; 113(3); 435-445.
- [55] De Carli F, Nobili L, Beelke M, Watanabe T, Smerieri A, Parrino L, Terzano MG and Ferrillo F. Quantitative analysis of sleep EEG microstructure in the time-frequency domain. *Brain Research Bulletin* 2004 Jun; 63(5): 399-405.
- [56] Wahlberg P and Lantz G. Methods for robust clustering of epileptic EEG spikes, *IEEE Transactions on Biomedical Engineering* 2000 Jul; 47(7): 857-868.
- [57] Geva AB and Kerem DH. Forecasting generalized epileptic seizures from the EEG signal by wavelet analysis and dynamic unsupervised fuzzy clustering. *IEEE Transactions on Biomedical Engineering* 1998 Oct; 45(10): 1205-1216.
- [58] Liu HS, Zhang T and Yang FS. A multistage, multimethod approach for automatic

- detection and classification of epileptiform EEG *IEEE Transactions on Biomedical Engineering* 2002 Dec; 49(12): 1557-1566.
- [59] Blanco S, D'Attellis CE, Isaacson SI, Rosso OA and Sirne RO. Time-frequency analysis of electroencephalogram series. III. Gabor and wavelet transforms. *Physical Review E* 1996 Dec; 54(6): 6661-6672.
- [60] Al-Nashash HA, Paul JS, Ziai WC, Hanley DF and Thakor NV. Wavelet entropy for subband segmentation of EEG during injury and recovery. *Annals of Biomedical Engineering* 2003 Jun; 31(6): 653-658.
- [61] Gutierrez J, Alcantara R and Medina V. Analysis and localization of epileptic events using wavelet packets. *Medical Engineering & Physics* 2001 Nov; 23(9): 623-631.
- [62] Cardenas-Barrera J, Lorenzo-Ginori J and Rodriguez-Valdivia E. A wavelet-packets based algorithm for EEG signal compression. *Medical Informatics and the Internet in Medicine* 2004 Mar; 29(1): 15-27.
- [63] Gigola S, Ortiz F, D'Attellis CE, Silva W and Kochen S. Prediction of epileptic seizures using accumulated energy in a multiresolution framework. *Journal of Neuroscience Methods* 2004 Sep 30; 138(1-2):107-111.
- [64] Guler I and Ubeyli ED. Adaptive neuro-fuzzy inference system for classification of EEG signals using wavelet coefficients. *Journal of Neuroscience Methods* 2005 Jul 27.
- [65] Rosso OA, Figliola A, Creso J and Serrano E. Analysis of wavelet-filtered tonic-clonic electroencephalogram recordings. *Medical & Biological Engineering & Computing*

2004 Jul; 42(4): 516-523.

- [66] Melek WW, Lu Z, Kapps A and Fraser WD. Comparison of trend detection algorithms in the analysis of physiological time-series data. *IEEE Transactions on Biomedical Engineering* 2005 Apr; 52(4): 639-651.
- [67] Allen R and Smith D. Neuro-fuzzy closed-loop control of depth of anaesthesia. *Artificial Intelligence in Medicine* 2001 Jar-Mar; 21(1-3): 185-191.
- [68] Zhang XS and Roy RJ. Derived fuzzy knowledge model for estimating the depth of anesthesia. *IEEE Transactions on Biomedical Engineering* 2001 Mar; 48(3):312-323.
- [69] Huupponen E, Himanen SL, Varri A, Hasan J, Saastamoinen A, Lehtokangas M and Saarinen J. Fuzzy detection of EEG alpha without amplitude thresholding. *Artificial Intelligence in Medicine* 2002 Feb; 24(2): 133-147.
- [70] Palaniappan R, Paramesran R, Nishida S and Saiwaki N. A new brain-computer interface design using fuzzy ARTMAP. *IEEE Transactions on Neural Systems and Rehabilitation Engineering* 2002 Sep; 10(3): 140-148.
- [71] Ben Dayan Rubin DD, Baselli G, Inbar GF and Cerutti S. An adaptive neuro-fuzzy method (ANFIS) for estimating single-trial movement-related potentials. *Biological Cybernetics* 2004 Aug; 91(2): 63-75.
- [72] Yin H, Zeng Y, Zhang J and Pan Y. Application of adaptive noise cancellation with neural-network-based fuzzy inference system for visual evoked potentials estimation. *Medical Engineering & Physics* 2004 Jan; 26(1): 87-92.

[73] Bay OF and Usakli AB. Survey of fuzzy logic applications in brain-related researches.

Journal of Medical Systems 2003 Apr;27(2):215-223.

[74] Acharya U R, Faust O, Kannathal N, Chua T and Laxminarayan S. Non-linear analysis

of EEG signals at various sleep stages. *Computer Methods and Programs in*

Biomedicine 2005 Oct; 80(1): 37-45.

[75] Kelly SP, Lalor EC, Finucane C, McDarby G and Reilly RB. Visual spatial attention

control in an independent brain-computer interface. *IEEE Transactions on Biomedical*

Engineering 2005 Sep; 52(9):1588-1596.

[76] Isoglu-Alkac U, Keskindemirci G and Karamursel S. Auditory on- and off-responses

and alpha oscillations in the human EEG. *International Journal of Neuroscience* 2004

Jul; 114(7): 879-906.



[77] Mouraux A and Plaghki L. Single-trial detection of human brain responses evoked by

laser activation of A delta-nociceptors using the wavelet transform of EEG epochs.

Neuroscience Letters 2004 May; 361(1-3): 241-244.

[78] Strauss DJ, Delb W and Plinkert PK. Analysis and detection of binaural interaction in

auditory evoked brainstem responses by time-scale representations. *Computers In*

Biology and Medicine 2004 Sep; 34(6):461-477.

[79] Niessing J, Ebisch B, Schmidt KE, Niessing M, Singer W and Galuske RA.

Hemodynamic signals correlate tightly with synchronized gamma oscillations.

Science 2005 Aug 5;309(5736): 948-951.

[80] Williams P and West M. EEG responses to photic stimulation in persons experienced at meditation. *Electroencephalography and Clinical Neurophysiology* 1975 Nov; 39(5): 519-522.

[81] Zhang W, Zheng R, Zhang B, Yu W and Shen X. An observation on flash evoked cortical potentials and Qigong meditation. *American Journal of Chinese Medicine* 1993; 21(3-4):243-249.

[82] <http://www.doh.gov.tw/statistic/index.htm>; Statistical data from the Bureau of National Health Insurance, Department of Health, executive Yuan Taiwan, 2003.

[83] Akay M. Wavelets in biomedical engineering. *Annals of Biomedical Engineering* 1995 Sep-Oct; 23(5): 531–542.



[84] Wiklund U, Akay M, Morrison S and Niklasson U. Wavelet decomposition of cardiovascular signals for baroreceptor function tests in pigs. *IEEE Transactions on Biomedical Engineering* 2002 Jul; 49(7):651-661.

[85] Bruns A. Fourier-, Hilbert- and wavelet-based signal analysis: are they really different approaches? *Journal of Neuroscience Methods* 2004 Aug; 137(2): 321-332.

[86] Graimann B, Huggins JE, Levine SP and Pfurtscheller G. Toward a direct brain interface based on human subdural recordings and wavelet-packet analysis. *IEEE Transactions on Biomedical Engineering* 2004 Jun; 51(6):954-962.

[87] Hafner HM, Brauer K, Eichner M, Steins A, Mohrle M, Blum A and Junger M.

- Wavelet analysis of cutaneous blood flow in melanocytic skin lesions. *Journal of Vascular Research* 2005 Jan-Feb; 42(1): 38-46.
- [88] Aldroubi A and Unser M: (Eds.): *Wavelets in medicine and biology*. CRC, Boca, Raton 1996.
- [89] Special issue on wavelets and signal processing. *IEEE Transactions on Signal Processing* 1993 Dec; 41(12): 3213-3600.
- [90] Special issue on wavelet transforms and multiresolution signal analysis. *IEEE Transactions on Information Theory* 1992 Mar; 38(2): 529-924.
- [91] Osowski S and Linh TH. ECG beat recognition using fuzzy hybrid neural network. *IEEE Transactions on Biomedical Engineering* 2001 Nov; 48(11):1265-1271.
- [92] Kwak KC and Pedrycz W. Face recognition using fuzzy integral and wavelet decomposition method. *IEEE Transactions on System Man and Cybernetics Part B-Cybernetics* 2004 Aug; 34(4): 1666-1675.
- [93] Yue X, Ye D, Zheng C and Wu X. Neural networks for improved text-independent speaker identification. *IEEE Engineering in Medicine and Biology Magazine* 2002 Mar-Apr; 21(2):53-58.
- [94] Hathaway RJ, Bezdek JC and Pal NR. Sequential Competitive Learning and the Fuzzy C-Means Clustering Algorithms. *Neural Networks* 1996 Jul; 9(5):787-796.
- [95] Akay M and Mulder EJ. Effects of maternal alcohol intake on fractal properties in human fetal breathing dynamics. *IEEE Transactions on Biomedical Engineering* 1998 Sep; 45:1097-1103.

- [96] Wornell GW and Oppenheim AV. Estimation of fractal signals from noisy measurements using wavelets. *IEEE Transactions on Signal Processing* 1992; 40:611–623.
- [97] Wornell GW and Oppenheim AV. Wavelet-based representations for a class of self-similar signals with applications to fractal modulation. *IEEE Transactions on Information Theory* 1992; 38: 785–800.
- [98] Wu Jue Miao Tian. *Diamond Sutra* (Chinese). Zen Cosmos Publish Ltd., Taiwan, 2004,
- [99] Barlow JS. *The Electroencephalogram: Its Patterns and Origins*. The MIT Press, Cambridge, MA: A Bradford Book, 1993.
- [100] Delorme A and Makeig S. EEGLAB: an open source toolbox for analysis of single-trial EEG dynamics. *Journal of Neuroscience Methods* 2004 Mar; 134(1):9-21.

Appendix-A: original survey questionnaires (Chinese version)

『禪修印心佛法』同修健康狀況調查表

各位親愛的師姐師兄：

爲了研究禪修對身體健康狀況之影響，懇請各位撥空填寫此問卷，協助本實驗室完成調查，感激不盡！

● 個人資料

年齡：_____

性別：男性，女性

婚姻：已婚，未婚

居住地：(1：台北 2：桃竹苗 3：中彰投 4：雲嘉南 5：高屏澎 6：宜蘭 7：花東) _____

教育程度：(1：國中小 2：高中職 3：大專 4：碩博士) _____

● 禪修狀況

➤ 禪修年數：_____年_____月

➤ 每次可禪修時間（請選擇自己禪坐狀況較好時的情形，請只填一項）

雙盤_____分鐘；單盤_____分鐘；如意盤_____分鐘

➤ 平均每週禪坐次數：每週_____次

➤ 近一年來平均每月至禪室上課_____次

➤ 自認爲禪修精進努力程度（請填寫數字 1~5，1：非常精進；2：堪稱精進；3：普通；4：不精進；5：非常不精進）_____

➤ 自認爲禪修在生命中所佔的重要程度（請填寫數字 1~5，1：非常重要；2：堪稱重要；3：普通；4：不重要；5：非常不重要）_____

● 影響健康之行爲分佈

➤ 過去一年中，有抽菸者請填寫下方空格（0：不抽菸 1：抽非常多煙 2：常抽菸 3：普通 4：不常抽菸 5：極少抽菸）_____

➤ 過去一年中，有喝酒者請填寫下方空格（0：不喝酒 1：喝酒非常嚴重 2：常喝酒 3：普通 4：不常喝酒 5：極少喝酒）_____

➤ 過去一年中，平均每週運動次數（每次運動需 30 分鐘以上）_____

➤ 過去一年中，平均睡眠情況（1：時常熬夜 2：偶爾熬夜 3：正常睡眠）_____

● 身體狀況

- 你認為自己目前健康狀況 (1: 非常好 2: 尙佳 3: 普通 4: 不好 5: 健康極差) _____
- 你認為自己目前健康狀況和一年前相比較 (1: 改善非常多 2: 有點改善 3: 一樣 4: 比較差 5: 更差) _____
- 你認為自己身體健康改善狀況與禪修前相比 (1: 改善非常多 2: 有點改善 3: 一樣 4: 比較差 5: 更差) _____
- 您在過去一年中 (2002 年 1 月至 12 月) 健保卡使用總格數 (例如: 一卡有六格, 用完 A 卡就有 6 格, 用到 B 卡 2 格就填 8 格) _____ 格
- (承接上題) 在過去一年中, 您最常就診的科別是: (1 內科 2 外科 3 皮膚科 4 眼科 5 牙科 6 耳鼻喉科 7 婦產科 8 神經內科 9 整形外科 10 精神科 11 其他) _____
- 您在過去一年中住院天數: _____ 天

● 心理健康狀況

- 您認為自己目前內心快樂感受的狀態為 (1: 非常快樂 2: 尙佳 3: 普通 4: 不好 5: 極差) _____
- 您認為自己目前心理的健康狀態和一年前比較 (1: 改善非常多 2: 有點改善 3: 一樣 4: 比較差 5: 更差) _____
- 過去一年中, 您認為外在生活壓力的程度 (1: 幾乎沒有壓力 2: 有點壓力 3: 普通 4: 壓力大 5: 壓力非常大) _____
- 過去一年中, 您認為自己面對生活壓力的能力如何 (1: 輕鬆面對 2: 尙可 3: 勉強應付得來 4: 不易調適自己面對生活壓力 5: 完全無法面對生活壓力) _____
- 與禪修前相比, 您認為自己目前內心快樂狀態 (1: 非常快樂 2: 比較快樂 3: 一樣 4: 比較差 5: 更差) _____

感恩各位師兄師姐的協助 祝大家 法喜充滿 共證菩提 謝謝